HAWC Detection of 100 TeV Gamma-ray Emission from the Pulsar Wind Nebula G32.64+0.53 (and brief outlook on ALP searches)

Youngwan Son, Chang Dong Rho, Ian James Watson,
Jason Sang Hun Lee, on behalf of the HAWC Collaboration

KSHEP-KPS Joint Workshop
November 20, 2025

Cosmic Rays & Knee

- Cosmic rays are charged particles ($e^-, e^+, p, \bar{p}$, heavier nuclei). Protons or nuclei are predominant.
- $\frac{dN}{dE} \propto E^{-\alpha}$
  - < ~4 PeV: $\alpha = 2.7$
  - > ~4 PeV: $\alpha = 3.1$
  - This break is called “knee.”
- One hypothesis to explain the knee is that **some sources can only accelerate hadrons around the knee, so-called “PeVatron.”**

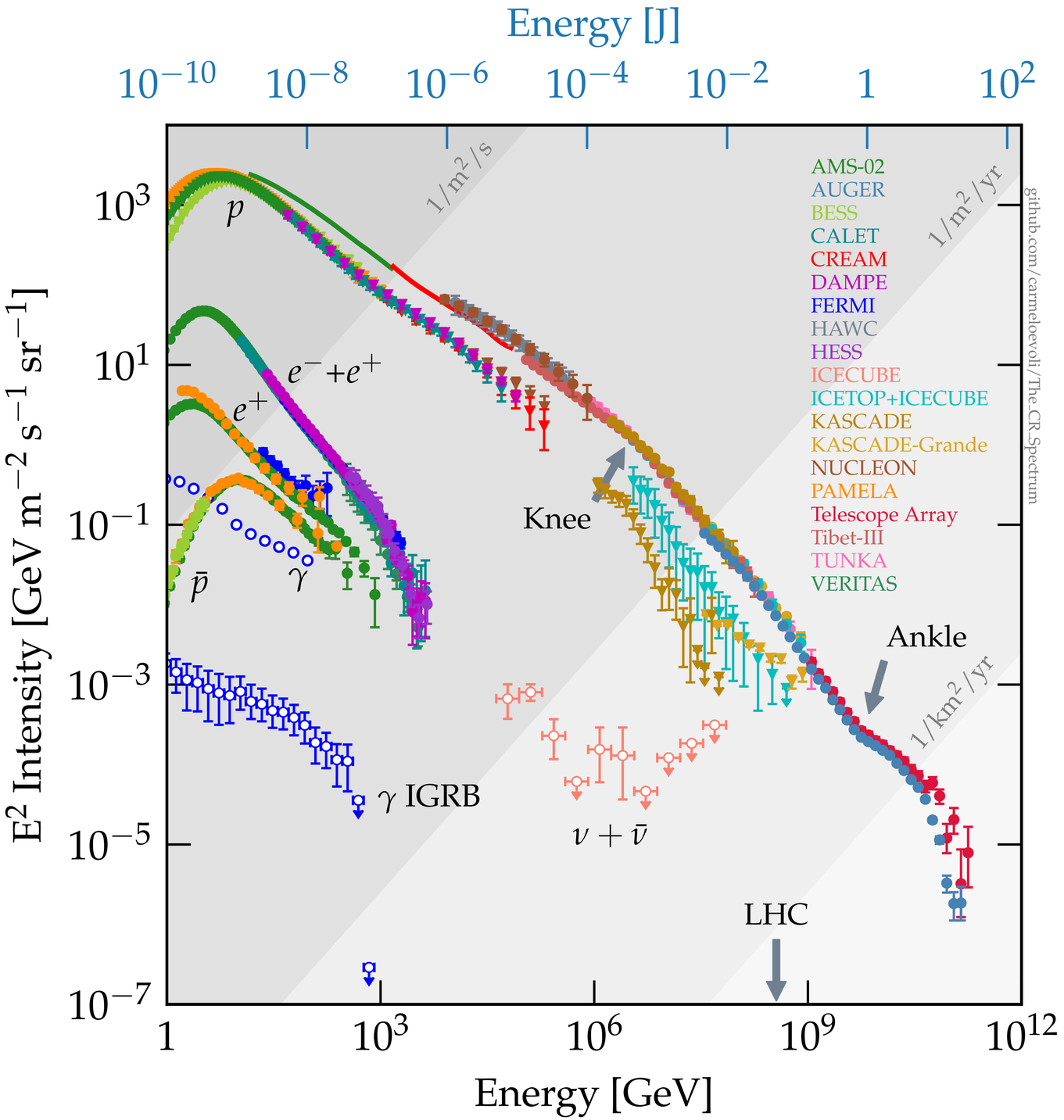

PeVatron Hunting

- However, finding PeVatron is difficult since direct observation is impossible because the magnetic field of the Milky Way deflects charged particles.

- But, we can use multi-TeV neutral particles (γ, ν) as a directional proxy of PeVatron, which the interaction of PeV particles and the surrounding medium can produce.

  - PeV protons -> ~0.1 PeV photons or neutrinos

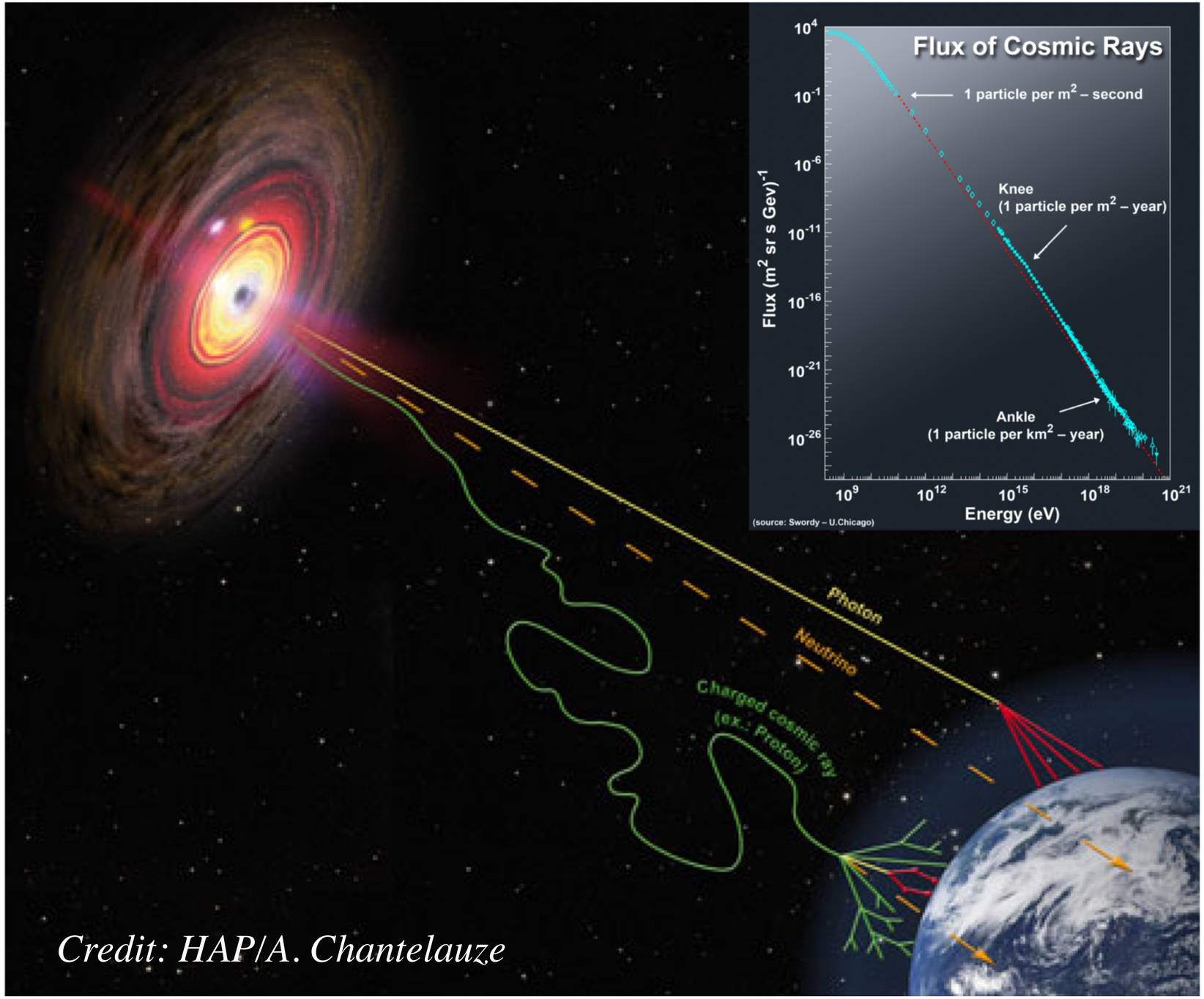

Leptonic Emissions

- However, PeVatron hunting is not simple because accelerated electrons can also produce TeV gamma rays through inverse Compton scattering.
- TeV astrophysical gamma rays result from the interplay between protons and electrons.
- Identifying origins and acceleration mechanisms is important to reveal or reject the PeVatron scenario for a given observation.
  - This can be identified by observing the leptonic signature - Klein-Nishina suppression in the multi-TeV spectrum.

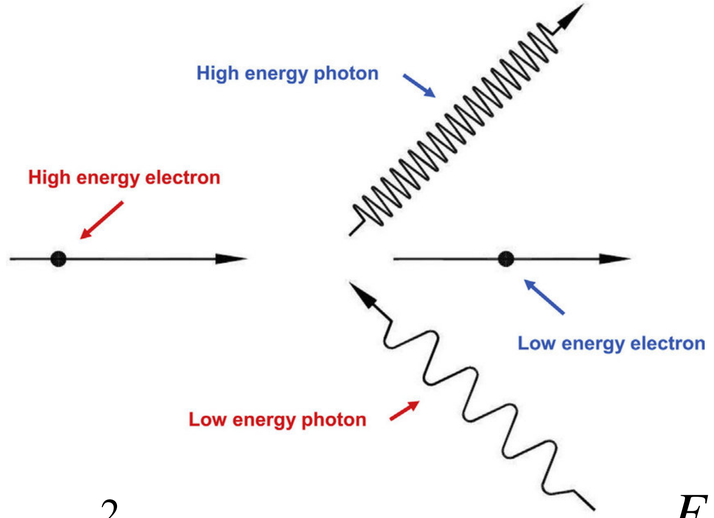

$$\sigma_{KN} = \frac{\pi r_e^2}{\alpha}\left(\ln(2\alpha) + 1/2\right) \qquad \alpha = \frac{E}{m_e c^2}$$

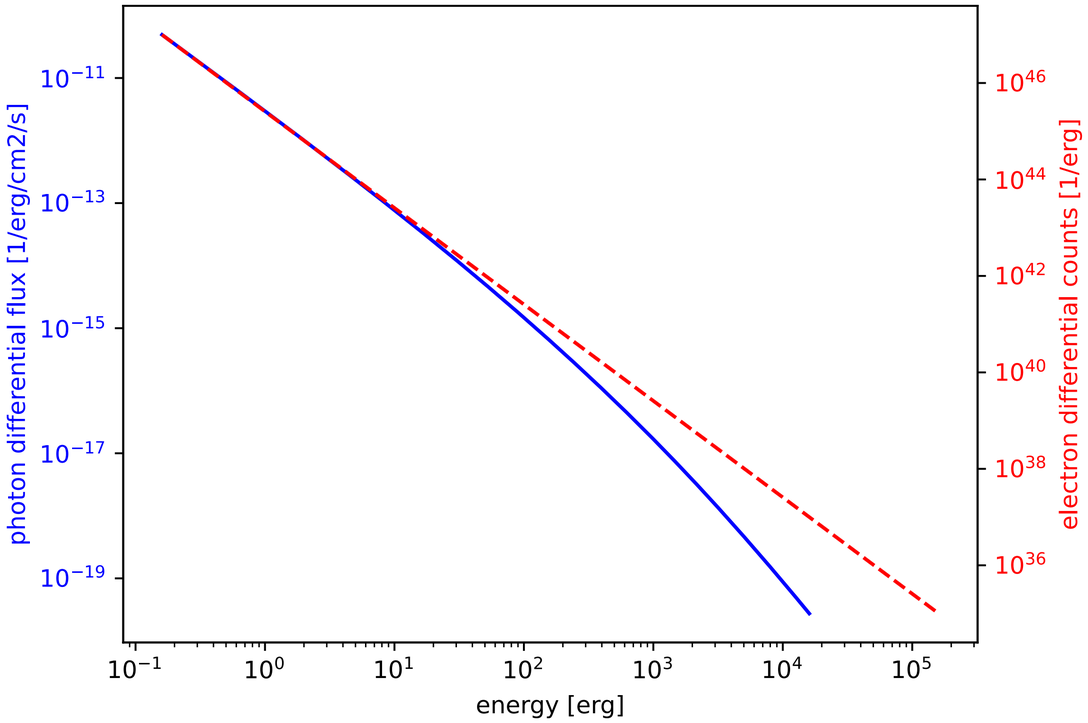

Detecting TeV photons

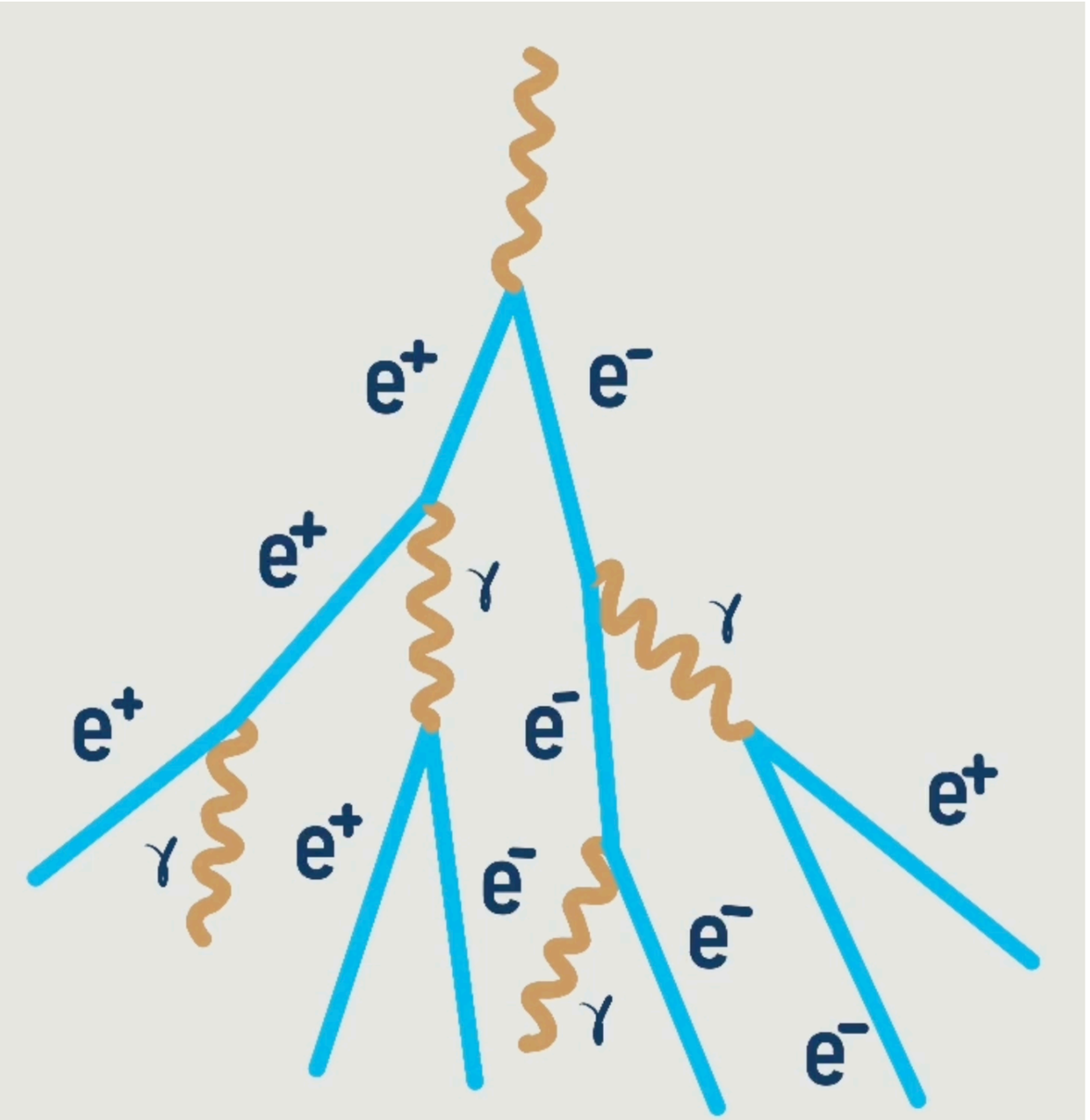

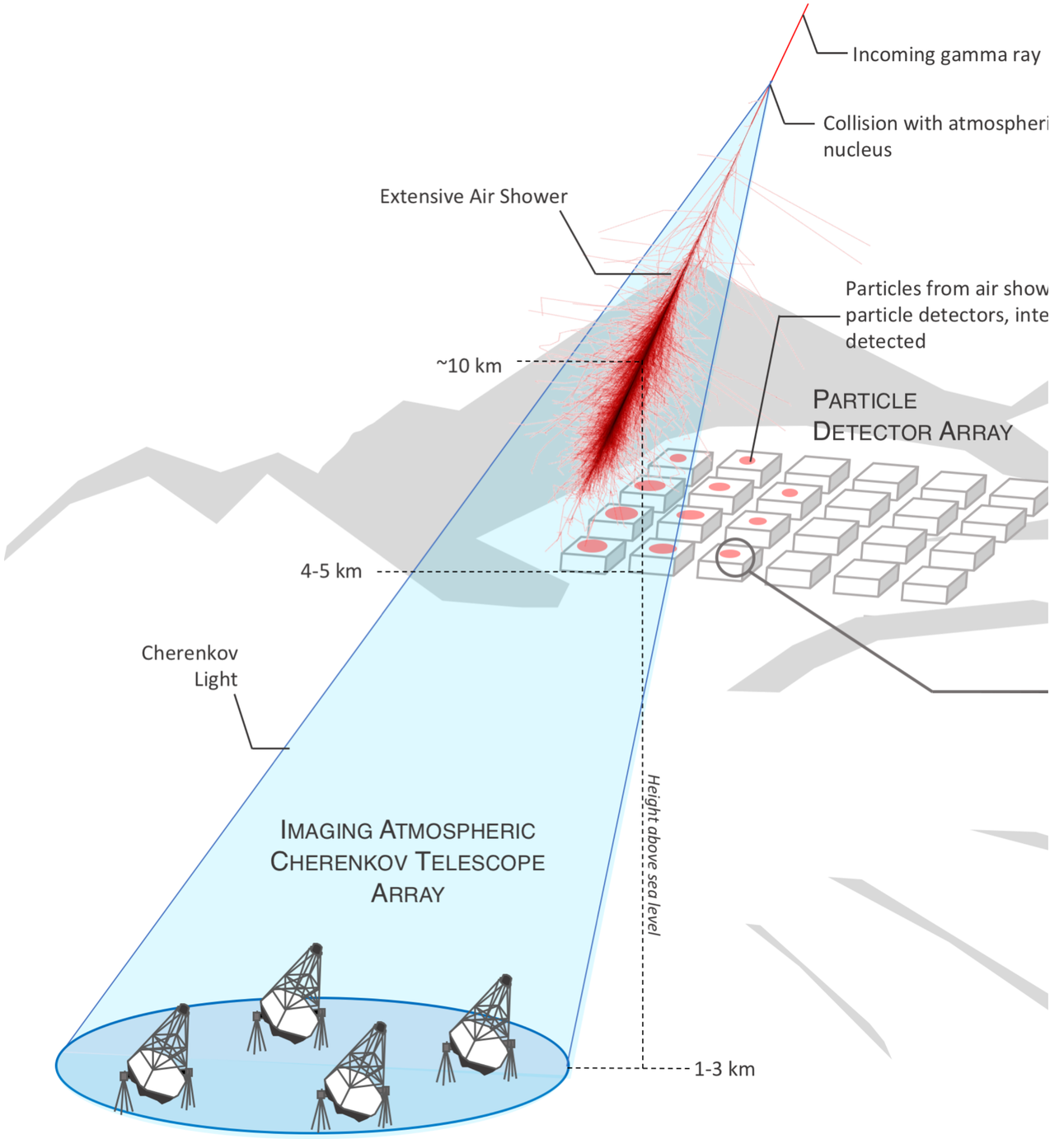

Shower image, 100 GeV γ-ray adapted from: F. Schmidt, J. Knapp, "CORSIKA Shower Images", 2005, https://www-zeuthen.desy.de/~jknapp/fs/showerimages.html

Detecting TeV photons

HAWC, Tibet ASgamma,

LHAASO, SWGO

HESS, MAGIC,
VERITAS, CTA

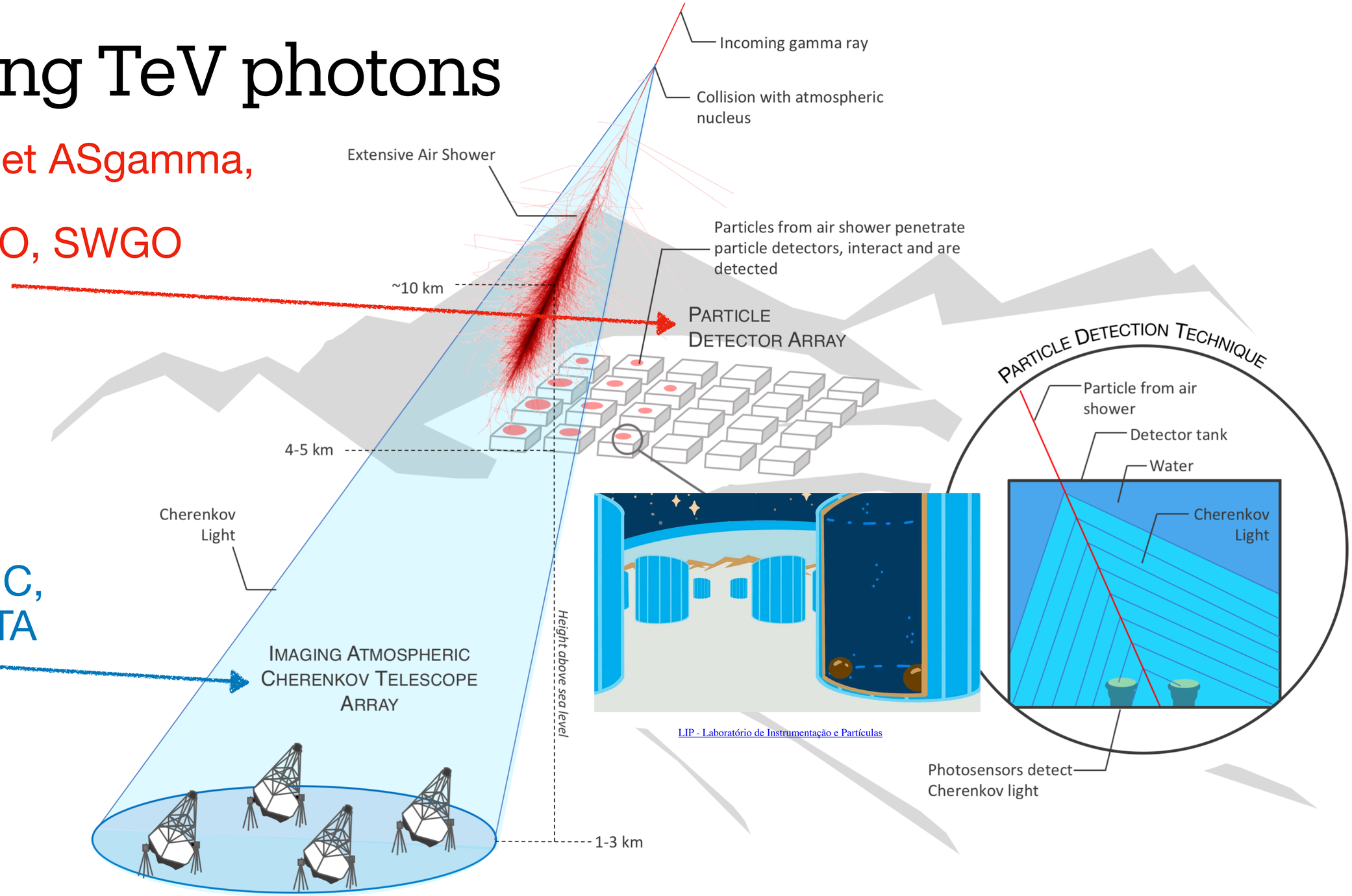

Shower image, 100 GeV γ-ray adapted from: F. Schmidt, J. Knapp, "CORSIKA Shower Images", 2005, https://www-zeuthen.desy.de/~jknapp/fs/showerimages.html

Not to scale

The HAWC Observatory

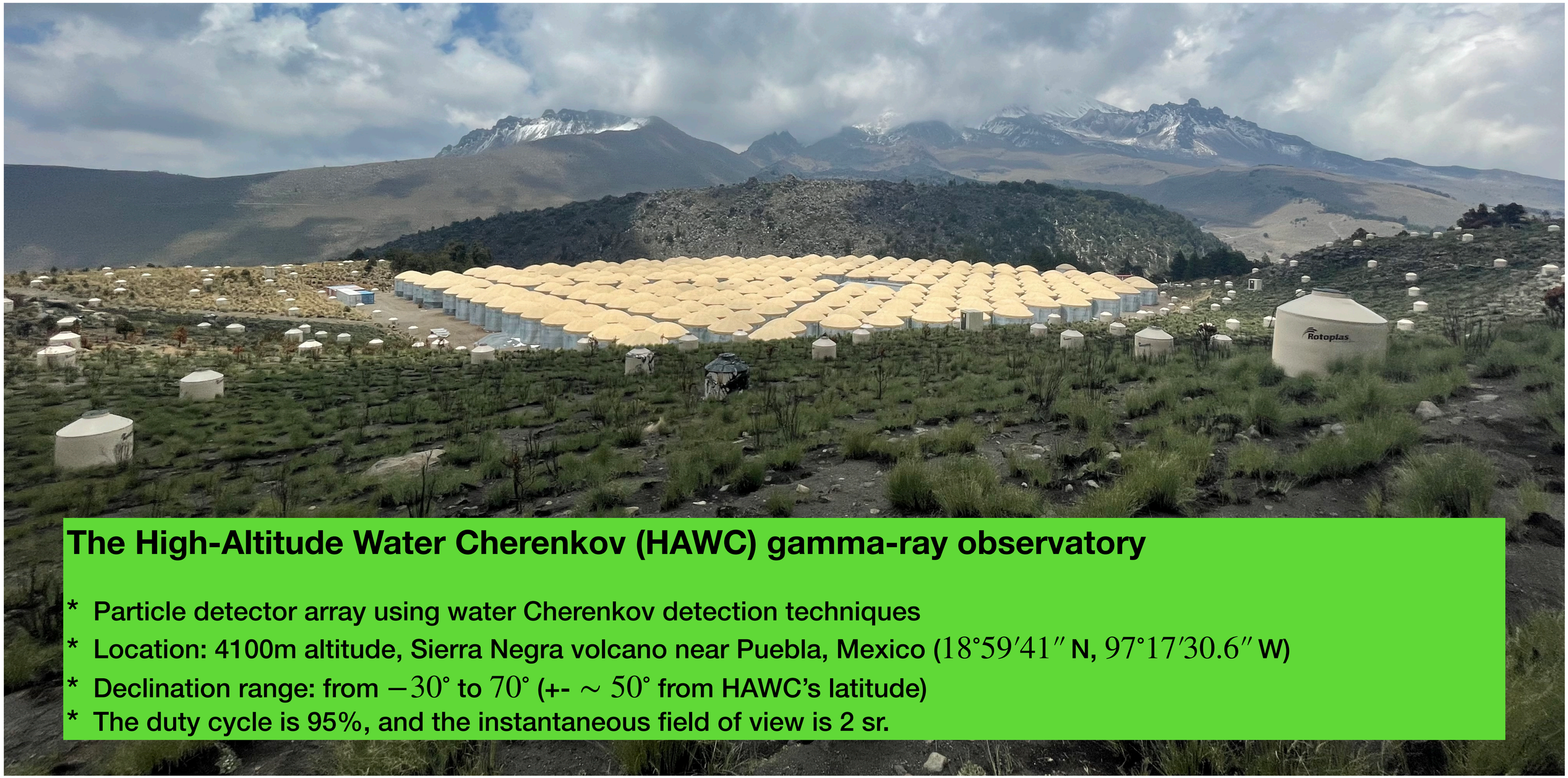

The High-Altitude Water Cherenkov (HAWC) gamma-ray observatory

* Particle detector array using water Cherenkov detection techniques
* Location: 4100m altitude, Sierra Negra volcano near Puebla, Mexico ($18°59'41''$ N, $97°17'30.6''$ W)
* Declination range: from $-30°$ to $70°$ (+- $\sim 50°$ from HAWC's latitude)
* The duty cycle is 95%, and the instantaneous field of view is 2 sr.

Ultra-High-Energy Sky

arXiv:1909.08609

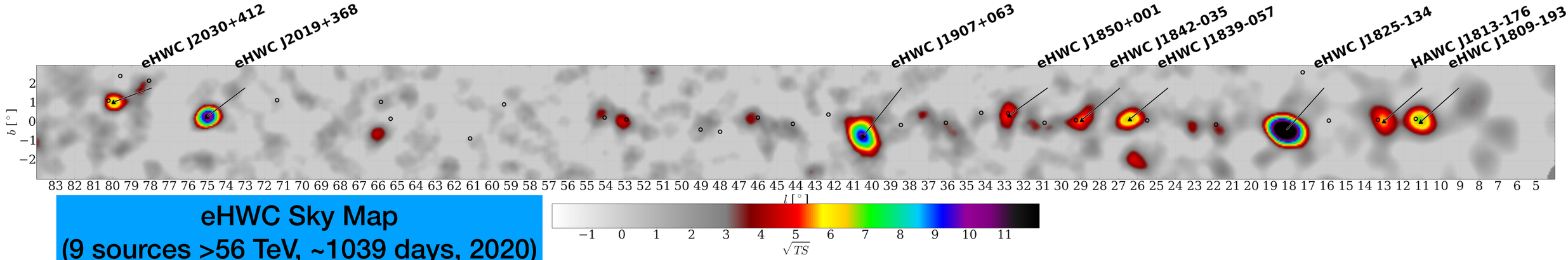

eHWC Sky Map
(9 sources >56 TeV, ~1039 days, 2020)

$$\mathrm{TS} = 2(\log(L_{\mathrm{Alt.}}) - \log(L_{\mathrm{Null}}))$$

arXiv:2305.17030

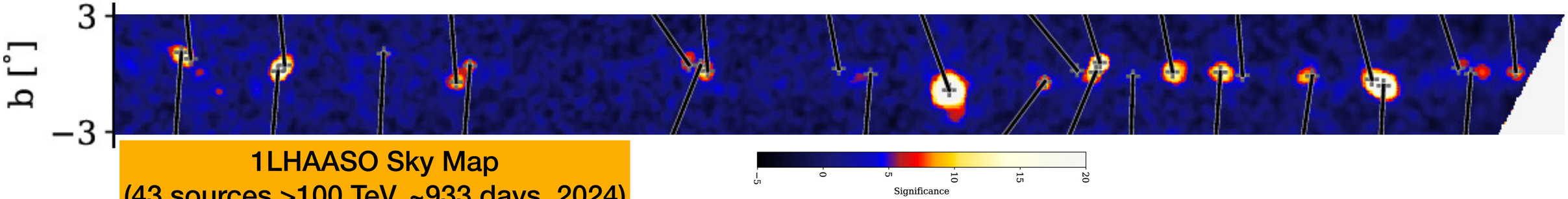

1LHAASO Sky Map
(43 sources >100 TeV, ~933 days, 2024)

- ~PeV protons -> ~100 TeV photons
- 100 TeV gamma ray sources -> PeVatron candidates

Up-to-date view

- Up-to-date view of the targets
- ~2860 days of data
- Improved reconstruction algorithms compared to the previous studies
- In the updated reconstructed data, the J1849 region exhibits significant emissions even at energies above 177 TeV.
  (maximum pre-trial σ = 7.27)
- The emissions are likely to be from eHWC J1850+001 (catalogued in 2019)
- Is it PeVatron? If not, what is that?

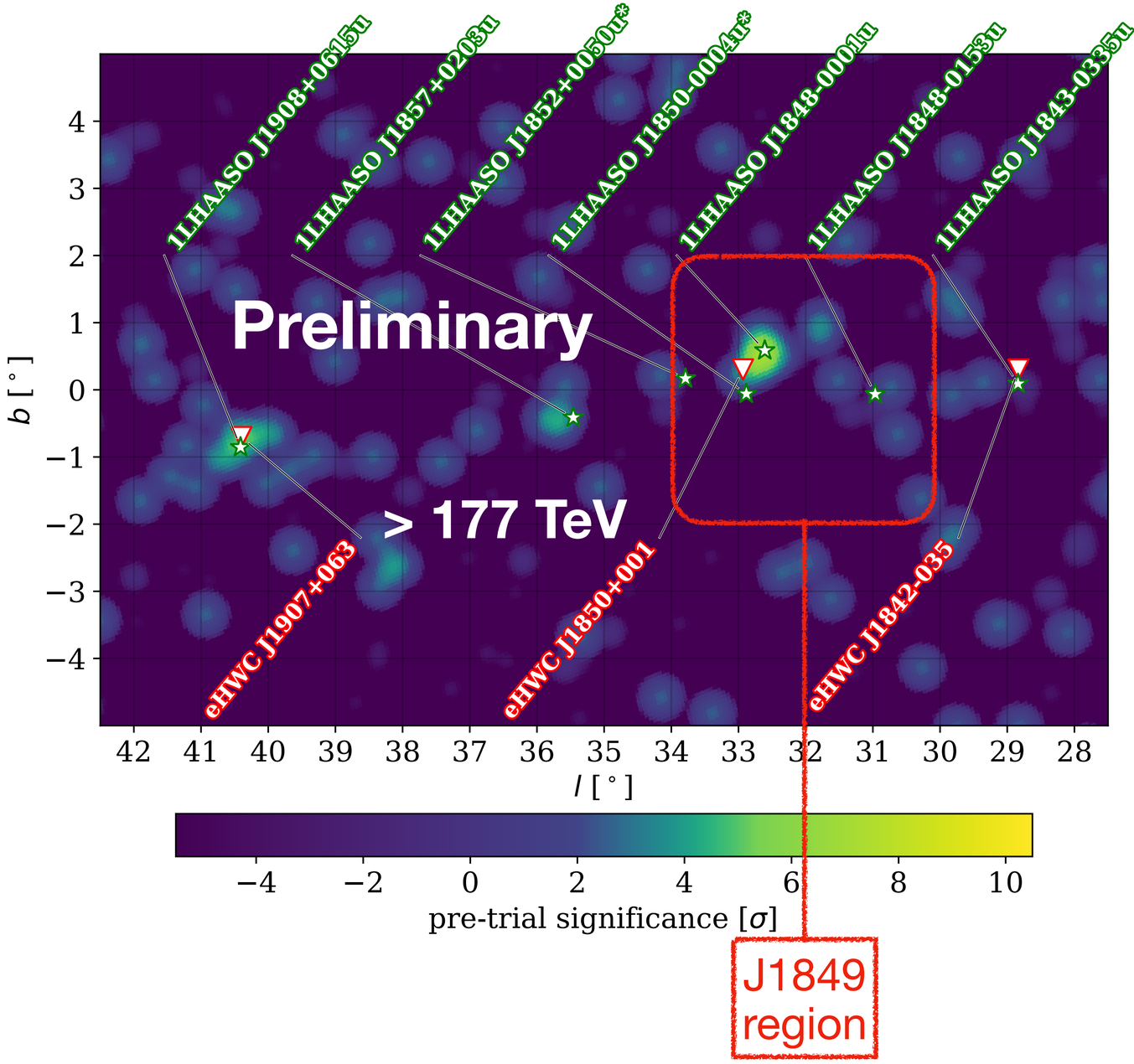

J1849 Region Analysis

~2860 days of observation

Reconstructed energy: 1-316 TeV

The region of Interest (ROI) is the brighter region.

There is a background emission throughout the entire Milky Way, known as galactic diffuse emission (GDE).

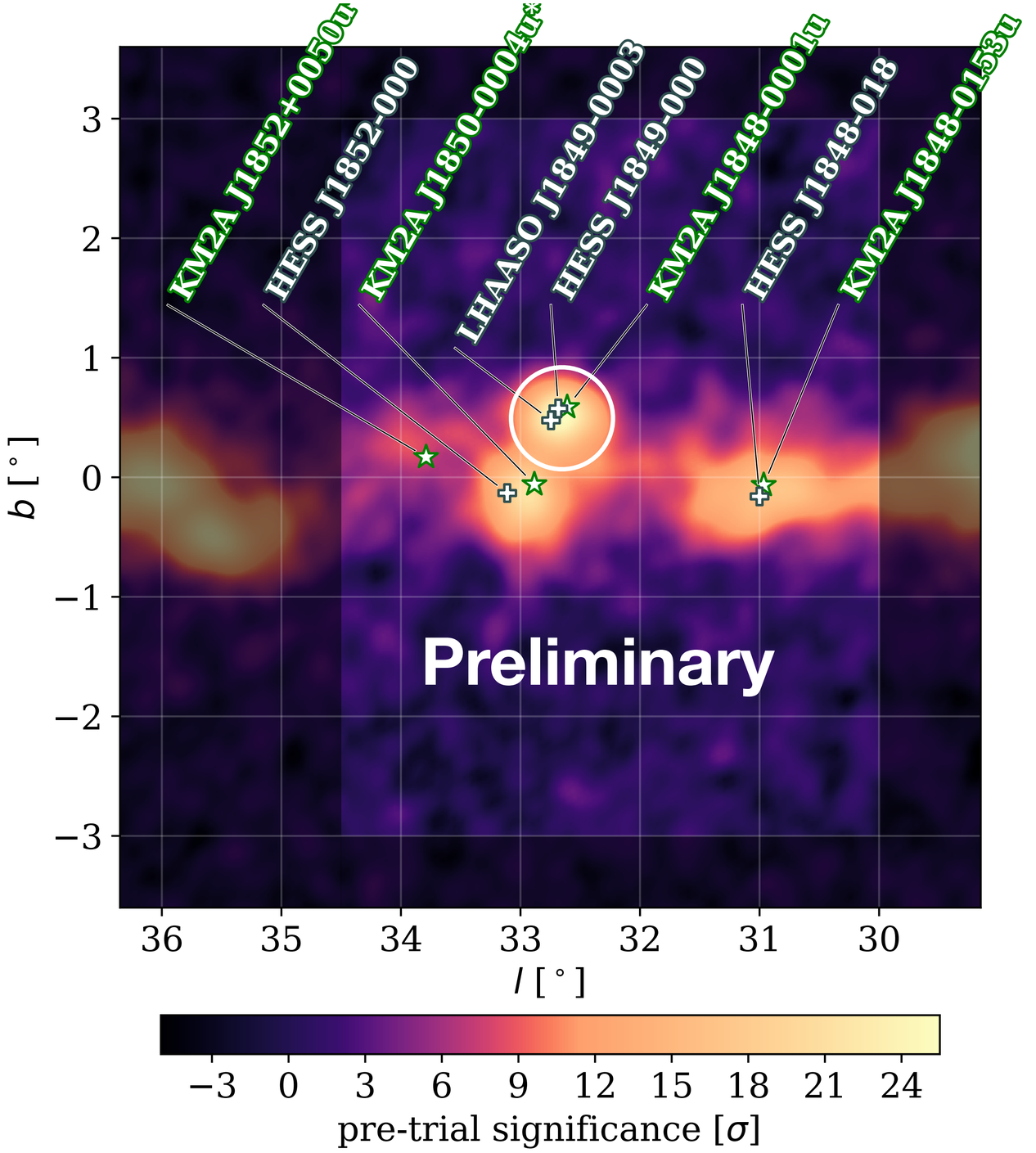

Galactic Diffuse Emission

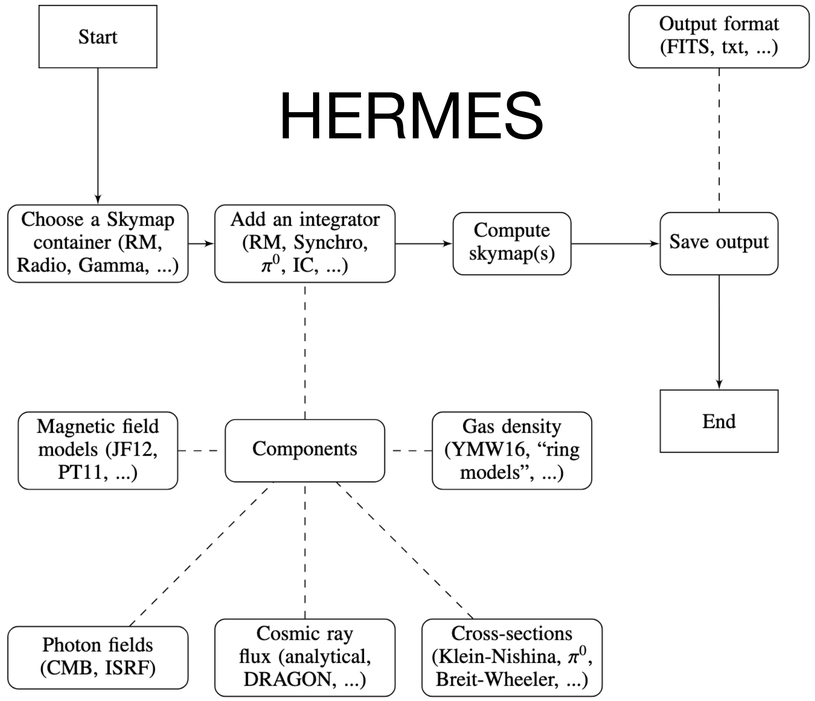

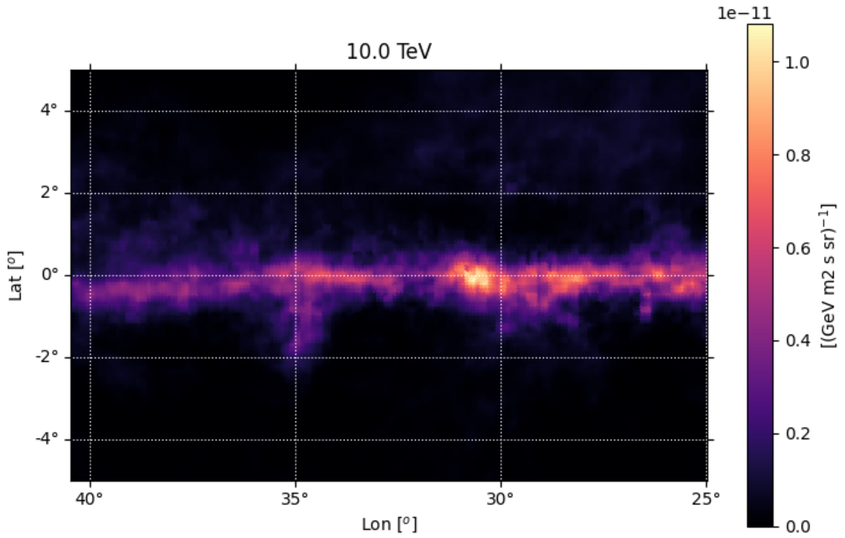

Hadronic - HI
(Neutral atomic H)

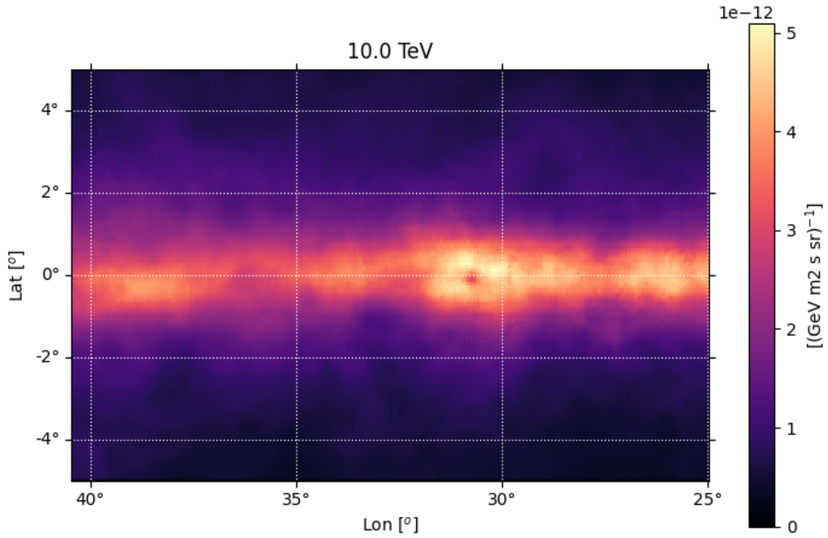

Hadronic - H_2

- Cosmic ray distributions are picked up from the DRAGON (cosmic ray propagation simulation).
- Hadronic (p-p collisions and neutral pion decays): Accelerated protons (their population from the simulation) collide with local gases (neutral atomic hydrogens (HI) and molecules (H_2)).
  - Note that the simulated cosmic ray distribution does not account for the inhomogeneous term. Therefore, I added a fitable scale factor with the GDE template.

Source Search Algorithm

arXiv:2407.10729

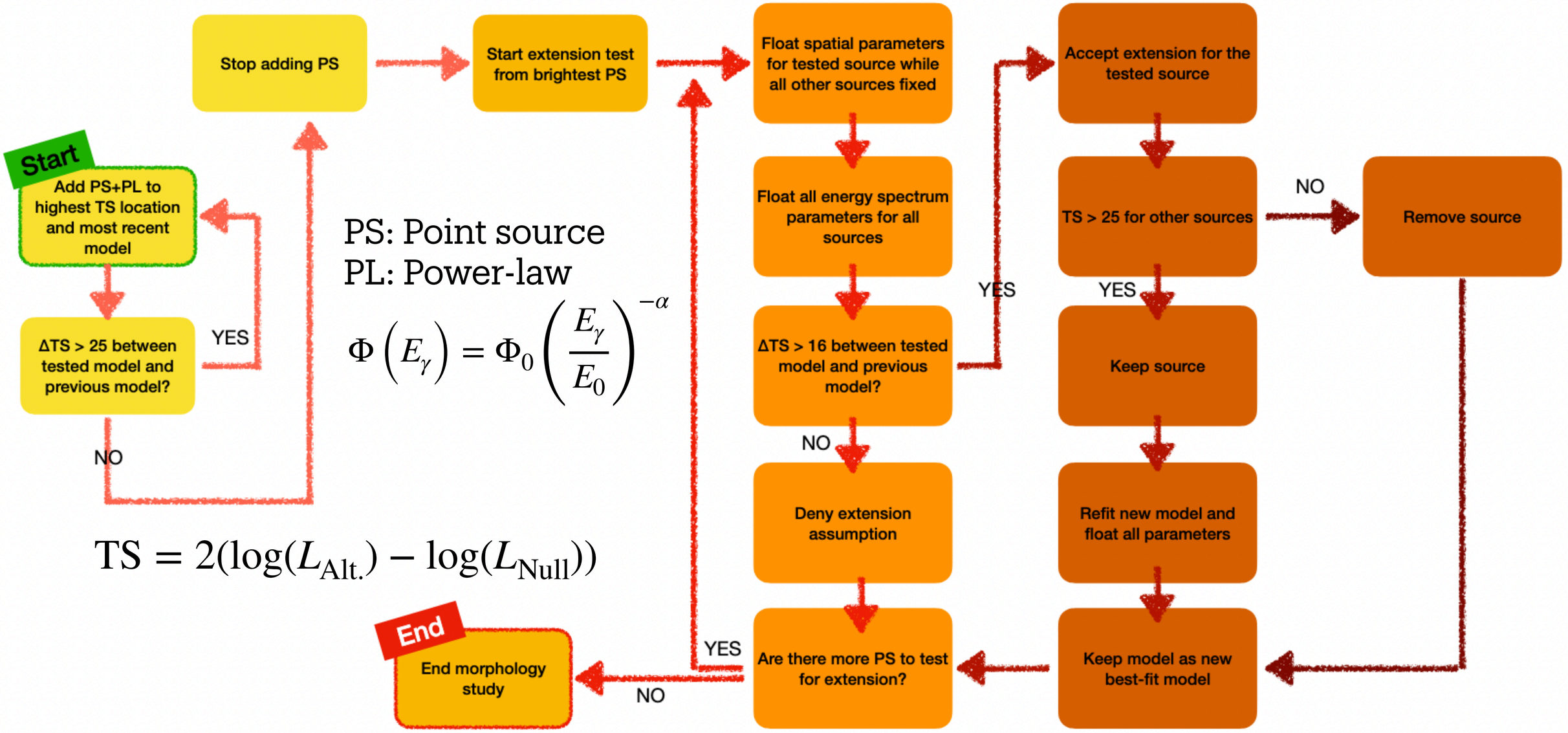

Final model

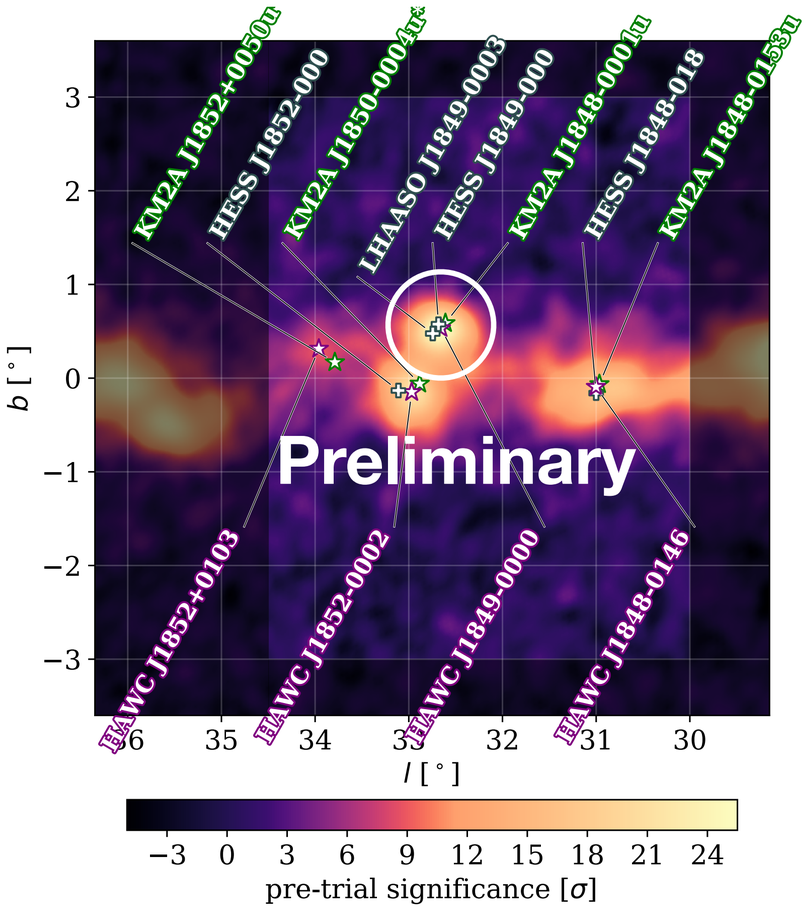

Data Map

−

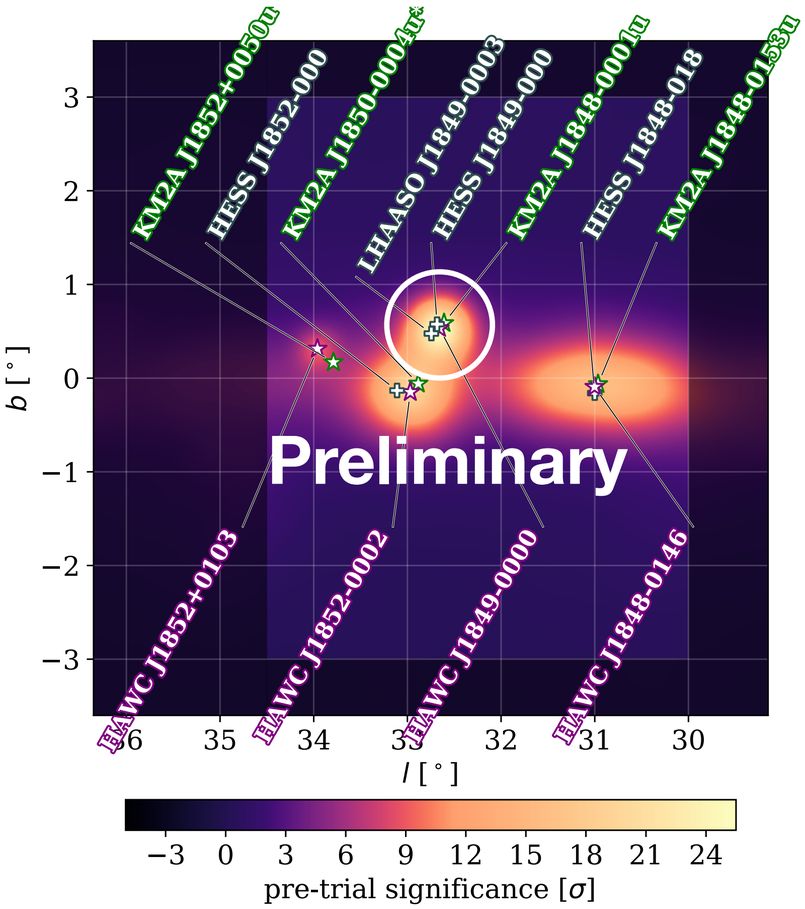

Model Map

=

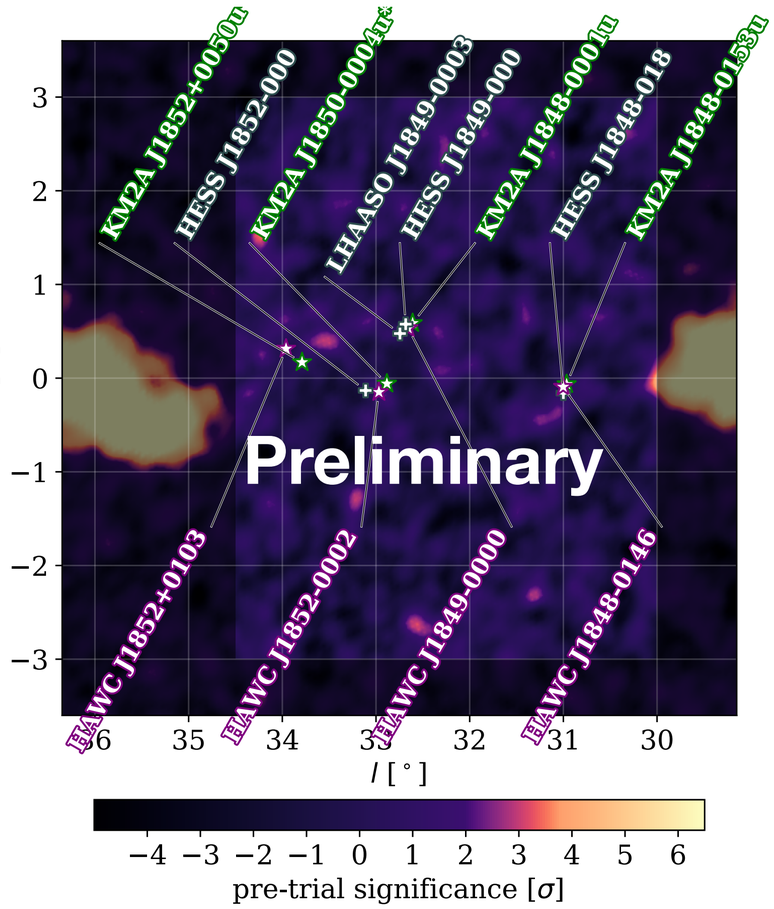

Residual Map

Spectrum of HAWC J1849-0000

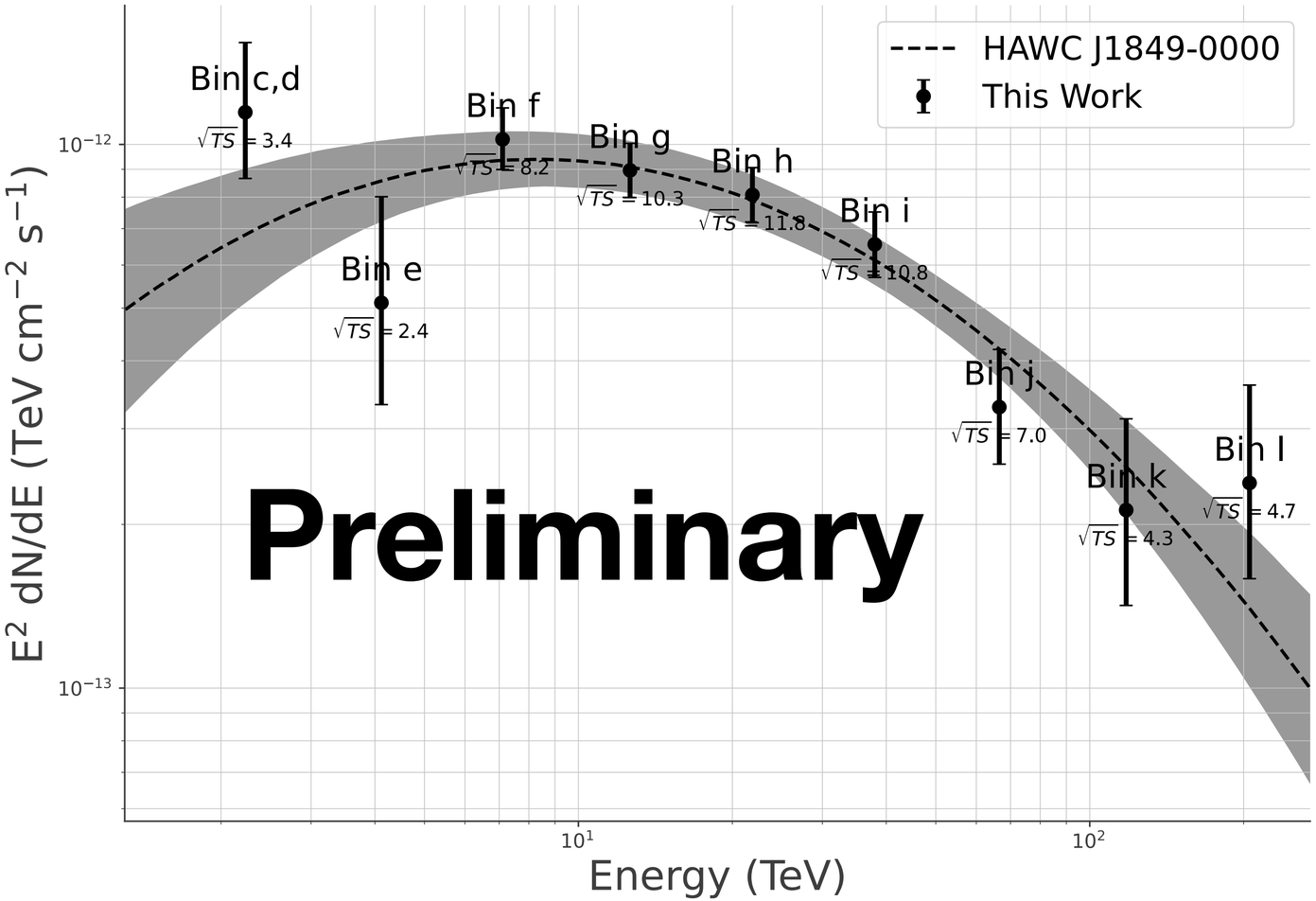

LogP spectrum: $\Phi\left(E_\gamma\right) = \Phi_0\left(\frac{E_\gamma}{10\ \mathrm{TeV}}\right)^{-\alpha-\beta\log\left(E_\gamma/10\ \mathrm{TeV}\right)}$

Fitted parameters (1 sigma error)

$\Phi_0 = 9.37^{+1.11}_{-0.99} \times 10^{-15}\ (\mathrm{TeV\ cm^2\ s})^{-1}$

$\alpha = 2.07^{+0.11}_{-0.11}$

$\beta = 0.19^{+0.06}_{-0.06}$

1 sigma spectrum bound: 1.3 - 270 TeV

The flux at each energy bin is computed by fitting Φ_0 while fixing the shape. ($\sqrt{\mathrm{TS}} \sim$ Significance)

The source is significant as four sigma at the highest energy bin (177-316 TeV)! -> Is it a PeVatron or not?

arXiv:2311.12376

Where these energetic photons come from

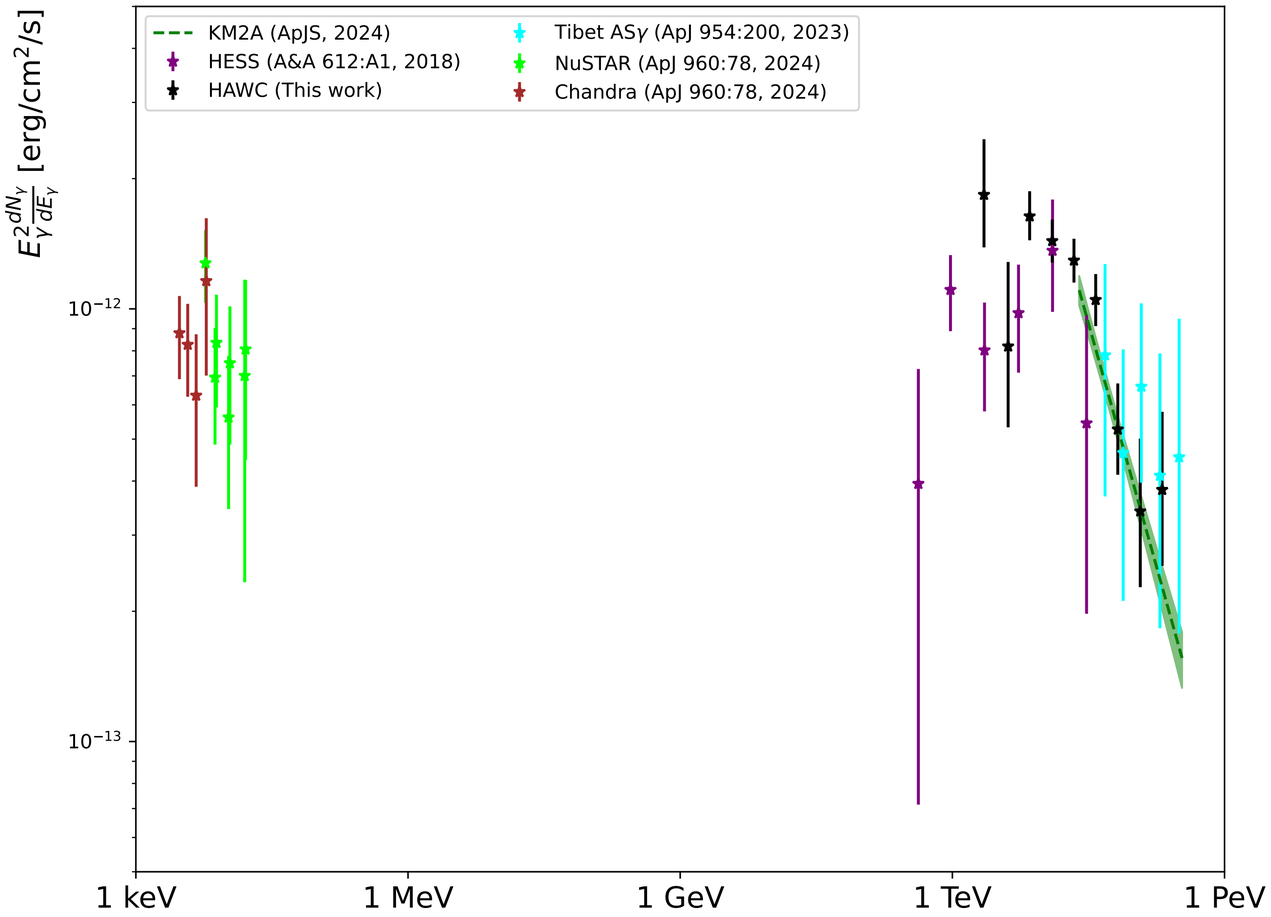

X-ray (keV)

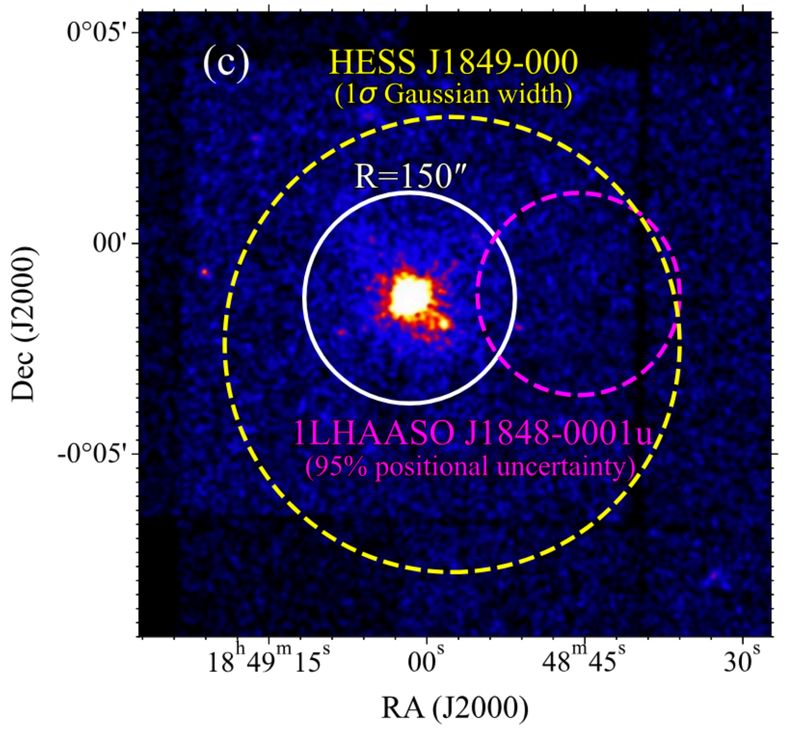

$P = 38.5$ ms

$\dot{P} = 1.4156 \times 10^{-14}$ s/s

PSR J1849-0001, one of the most energetic pulsars, is located nearby.

Its pulsar wind nebula (PWN) G32.64+0.53 is located within the TeV emissions observed by H.E.S.S. and LHAASO.

PWNe have been observed as a powerful electron accelerator. -> probably not a “hadronic” PeVatron

Pulsar basics

PSR

(Canonical pulsar assumption: $I = 10^{45}\ \mathrm{g\ cm^2}$)

Assume it is a rigid body (well, a pulsar is almost rigid). $E = \frac{I\Omega^2}{2} = \frac{2\pi^2 I}{P^2}$.

The derivative is $\dot{E} = I\Omega\dot{\Omega} = -\frac{4\pi^2 I\dot{P}}{P^3}$. -> A pulsar is losing energy by spinning down.

For a pulsar, P and $\dot{P}$ can be measured.

PSR J1849-0001: $P = 38.5\ \mathrm{ms},\ \dot{P} = 1.4156 \times 10^{-14}\ \mathrm{s/s}$ -> $\dot{E} = 9.6 \times 10^{36}\ \mathrm{erg/s}$

Assume the rotational energy ($\dot{E}$) is emitted through magnetic dipole radiation ($P = \frac{2}{3c^3}\dot{m}^2$) -> $\Omega \propto -\dot{\Omega}^3$

-> We know how the spin evolves ($\Omega \propto -\dot{\Omega}^3$), therefore, we can write $P(t)$, $\dot{E}(t)$, and $B(t)$.

PWN-powered Accelerator

PSR

Wind

Energies
&
Electrons

Accelerated
electrons

Spin-down power $\dot{E}$

Cooling

Inverse Compton scattering

CMB
IR & starlight
Synchrotron

TeV
gamma rays

Magnetic Field Synchrotron

Radio to X-ray

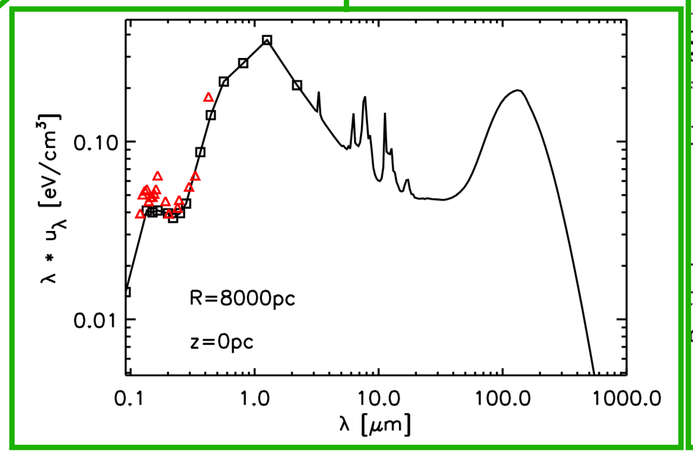

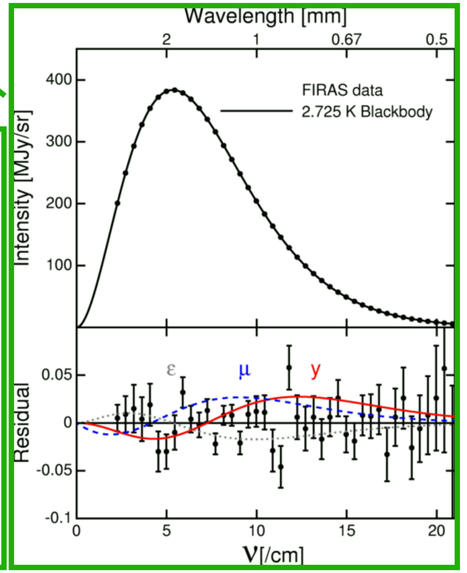

Pulsar-powered Accelerator

$P = 38.5$ ms
$\dot{P} = 1.4156 \times 10^{-14}$ s/s

* Rotation-powered, time-dependent

Age: $\tau = \frac{P}{2\dot{P}}\left(1 - \left(\frac{P_0}{P}\right)^2\right)$ Spin-down timescale: $\tau_0 = \frac{P_0^2}{2\dot{P}P}$

Time evolution:

$\dot{E}(t) = \dot{E}_0\left(1 + \frac{t}{\tau_0}\right)^{-2}$, $\dot{E}_0 = \dot{E}(\tau)\left(1 + \left(\frac{\tau}{\tau_0}\right)\right)^2$ <- P (obs.), $\dot{P}$ (obs.), P_0 (free)

-> A fraction of spin-down power $\eta\dot{E}(t)$ is used to accelerate electrons. <- η (free)

-> Determine a normalisation of the electron spectrum $F_e(E_e)$ <- α (free), $E_{\rm cutoff}$ (free)

$B(t) = B_0\left(1 + \sqrt{\frac{t}{\tau_0}}\right)^{-1}$, $B_0 = B(\tau)\left(1 + \sqrt{\frac{\tau}{\tau_0}}\right)$

$F_e(E_e) \propto \left(\frac{E_e}{1\ \text{TeV}}\right)^{-\alpha} \exp\left(-\frac{E_e}{E_{\rm cutoff}}\right)$

-> Synchrotron radiation and electron cooling. <- P (obs.), $\dot{P}$ (obs.), P_0 (free), $B(\tau)$ (free)

Free parameters: $P_0, \eta, B(\tau), \alpha, E_{\rm cutoff}$

Fitting Setup

$P = 38.5$ ms

$\dot{P} = 1.4156 \times 10^{-14}$ s/s

$R_{\mathrm{PWN}} = 5$ pc (Synchro Self-Compton)
[C. Kim et al. ApJ 960 (2024) 78]

$d = 7$ kpc
[E.V. Gotthelf et al. ApJL 729 (2011) 2 L16]

Photon seeds:

* CMB (2.7 K, 0.25 eV/cm^3)
* Interstellar Radiation Field (ISRF; IR, Starlight)
  [C.C. Popescu et al. MNRAS 470 (2017) 2539]

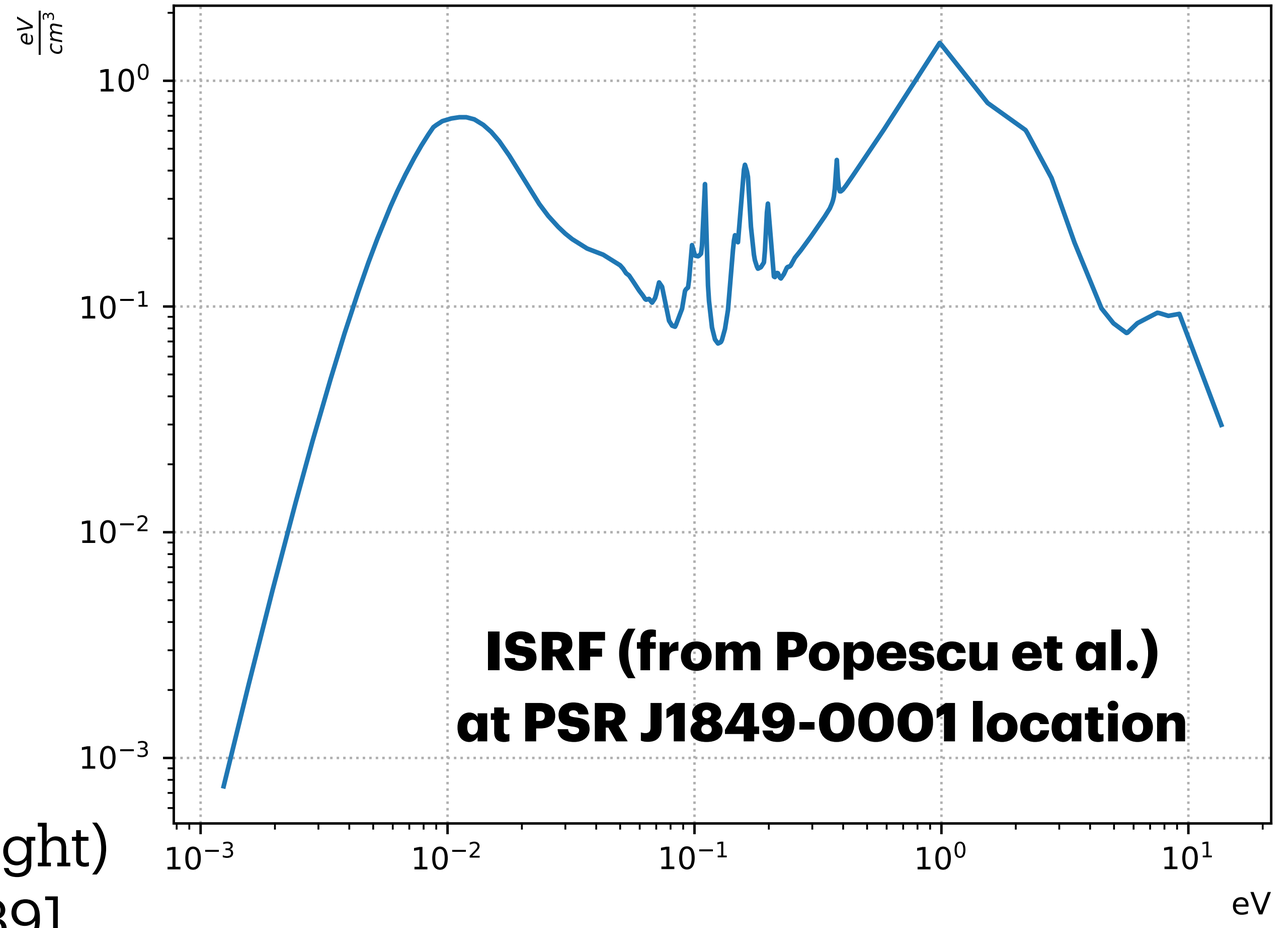

Fit Results

reported as (quantile $0.5\ ^{0.84}_{0.16}$)

Initial period [ms]: $23.7^{+2.4}_{-3.0}$

Conversion efficiency [%]: $1.2^{+1.1}_{-0.4}$

electron index: $1.82^{+0.14}_{-0.18}$

electron cutoff energy [PeV]: $1.5^{+1.7}_{-0.6}$

Current B-field [uG]: $2.50^{+0.13}_{-0.13}$

True age: 26.8 kyr

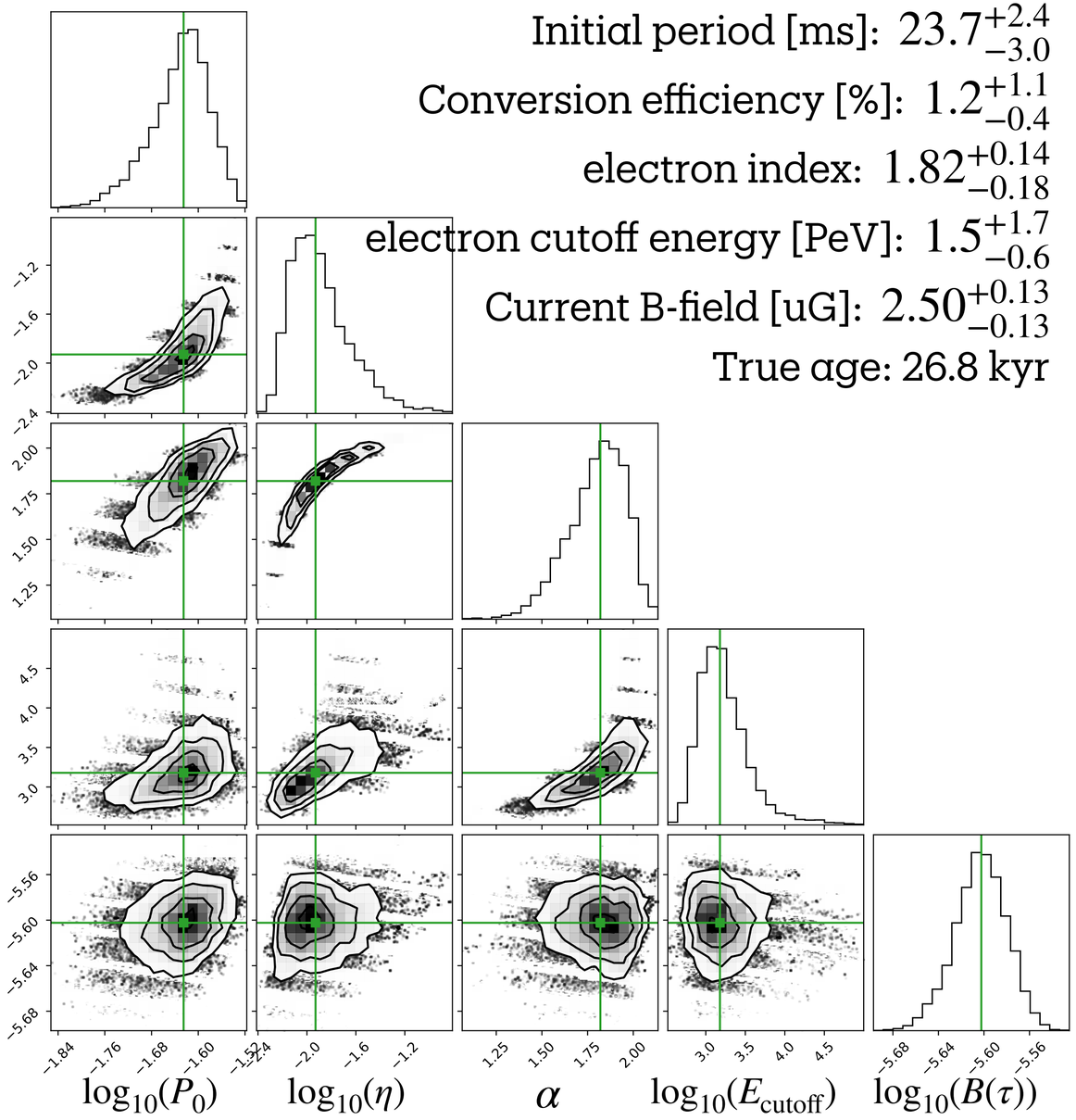

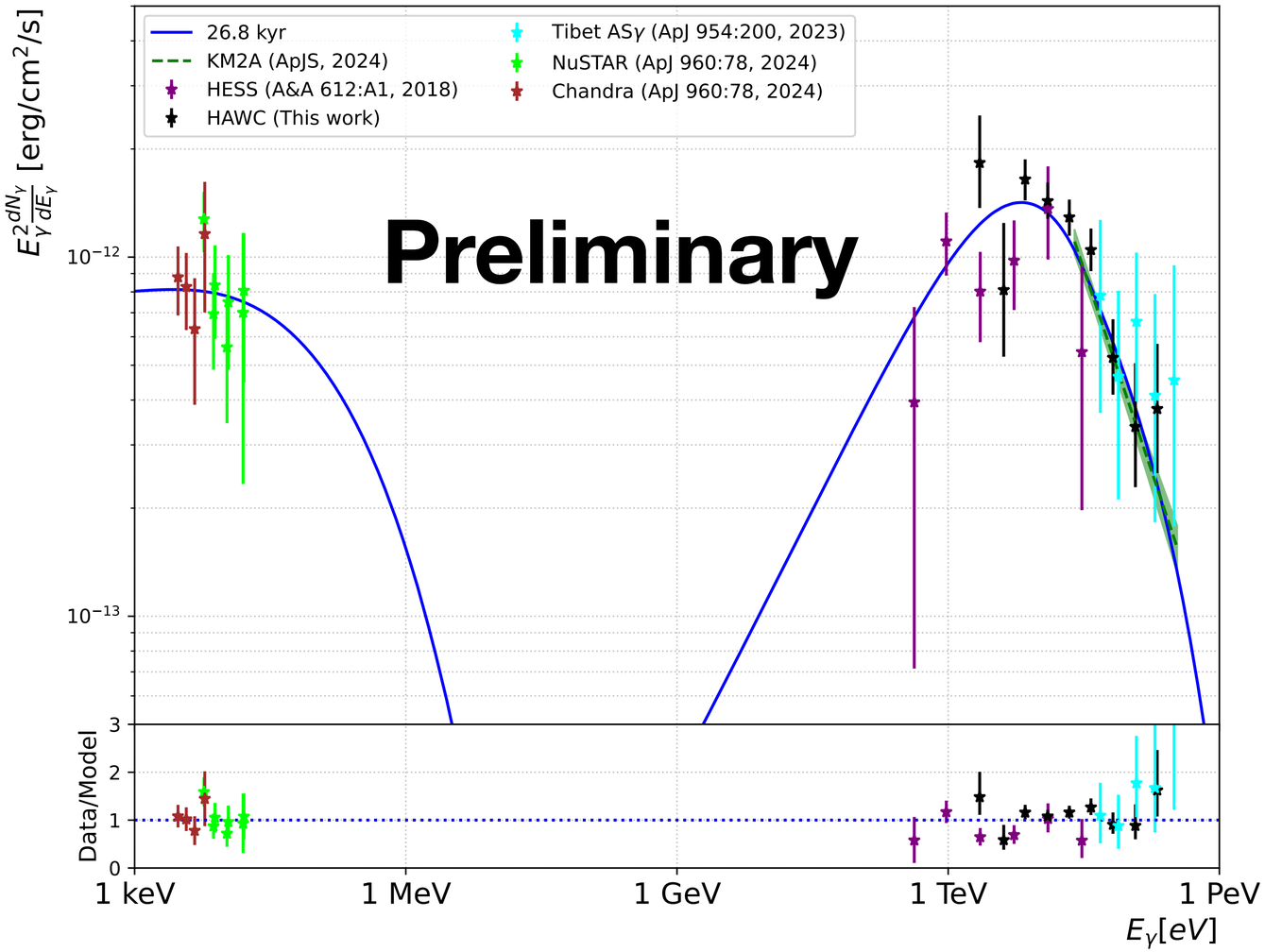

Paper is now under the collaboration reivew

Axion-like particles (ALPs)

$$L_{a\gamma\gamma} \propto g_{a\gamma\gamma} a F \tilde{F}$$

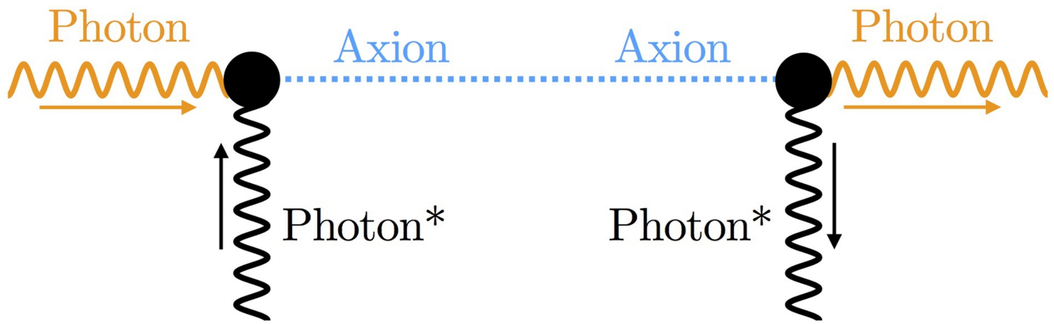

Axion-like particles are neutral pseudo-Goldstone bosons that arise from global U(1) symmetry.
Because of their low mass and weak interaction with the SM particles, they are regarded as candidates for WISP dark matter (Weakly Interacting Slim Particle).
The chiral anomaly leads to ALP-photon oscillation, which is a conversion between ALPs and photons in the presence of an external magnetic field. This oscillation presents an opportunity to discover ALPs.

22

Gamma-ray opacity and ALPs

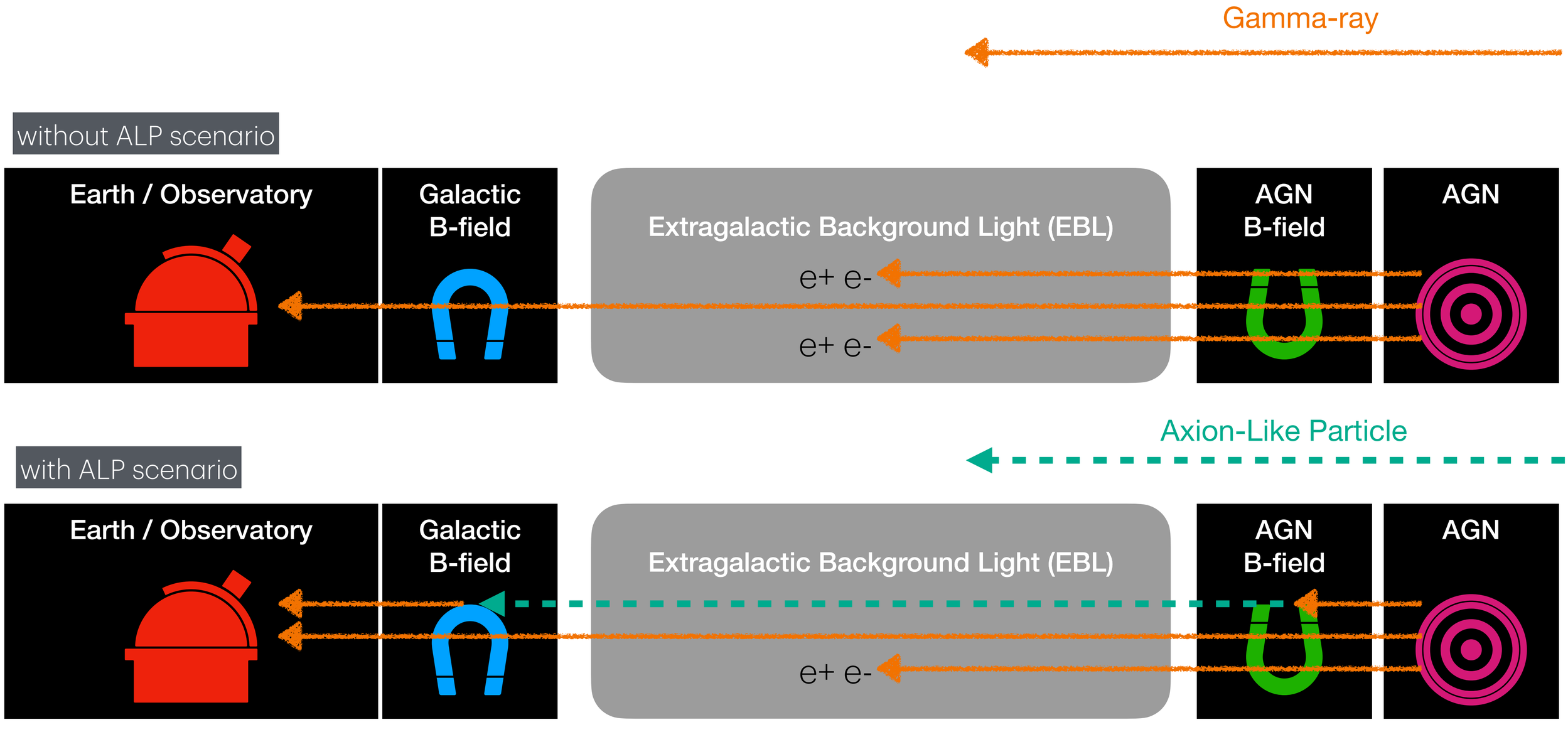

Three AGN of interest

Source	VER J0521+211	1ES 0229+200	PG 1553+113
redshift (z)	0.18	0.14	0.43
Blazar's B-field	Jet	ICMF	Jet+ICMF
$\theta_{\rm obs}^{\rm Jet}$ [°]	1.8	-	1.0
$B_0^{\rm Jet}$ [G]	0.1	-	0.5
$n_0^{\rm Jet}$ [10^3 cm^{-3}]	31.5	-	5.35
$r_{\rm VHE}^{\rm Jet}$ [10^{-3} pc]	26.0	-	63.0
$B_0^{\rm ICMF}$ [10^{-6} G]	-	3.5	1.0

Sources listed in the ALP search paper using HAWC public data (arXiv:2203.04332).

Selection based on:

* Located in the HAWC sky ($-10^\circ - 50^\circ$)
* Flux observation in 0.1 - 1 TeV (IACT)
* Not too variable (in GeV)

Among those blazars, we found that three blazars can be used to establish an exclusion space with the up-to-date HAWC data.

Photon survival probabilities

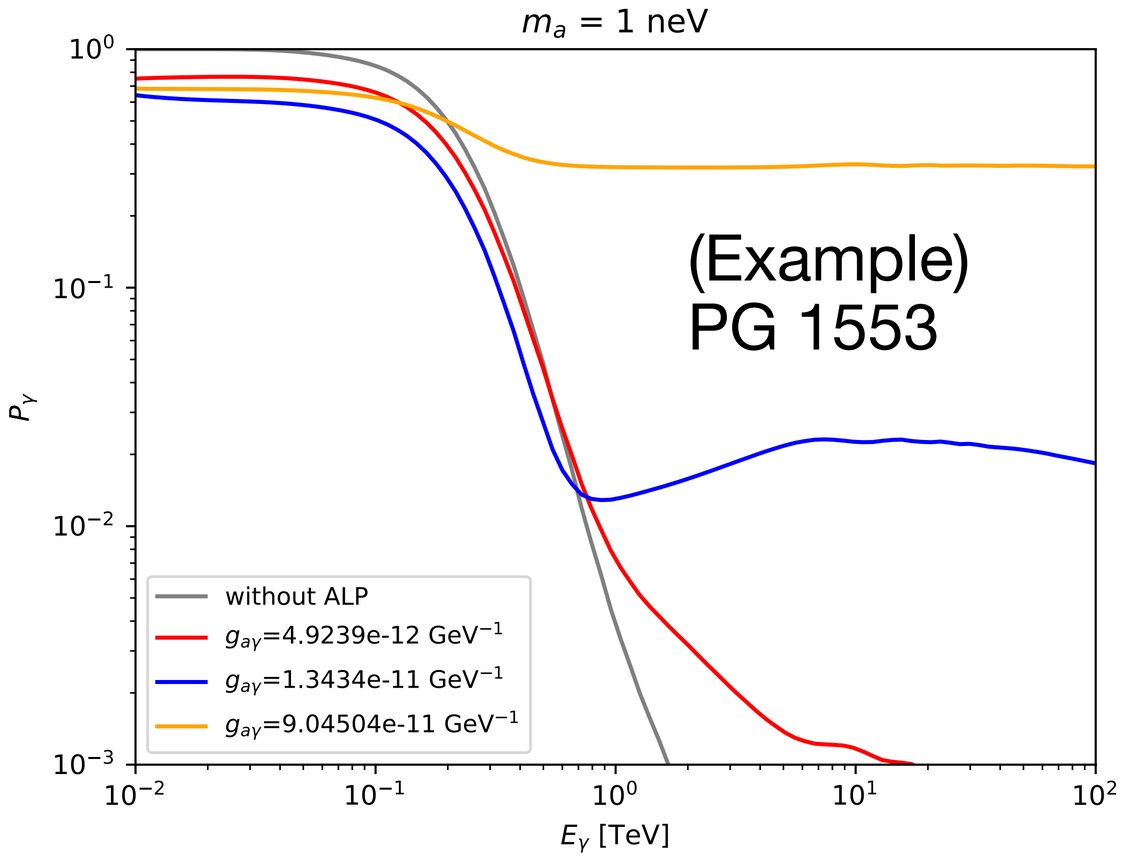

Simulate photon survival probabilities

$$P_\gamma(E_\gamma, m_a, g_{a\gamma\gamma}, z, B_{\rm src}, B_{\rm GMF})$$

Planck's Estimate
arXiv:1601.00546

Gamma-ray ALP

Source	1ES 0229	PG 1553
R.A.(J2000)	02h32m53.2s	15h55m44.7s
Dec.(J2000)	+20d16m21s	+11d11m41s
z	0.14	≥ 0.4
Var. index [67]	6.799	107.2
Data	H.E.S.S [61]	VERITAS
B-field scenario	ICMF+GMF	Jet+ICMF+GMF
B_0^{Jet} [G]		0.5
n_0^{Jet}		5.35×10^3
β^{Jet}		2
δ		35
$\theta_{\rm obs}$		1°
$r_{\rm VHE}$ [pc]		0.063
$r_{\rm max}$ [kpc]		1

$$P_\gamma = \frac{N_\gamma^{\rm Earth}}{N_\gamma^{\rm AGN}}$$

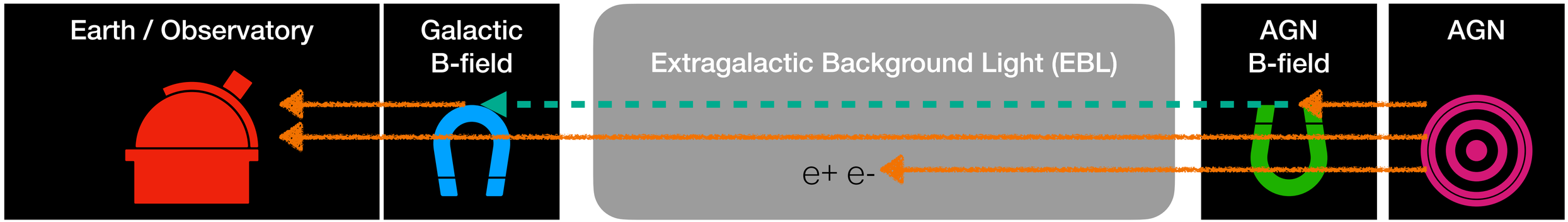

Fitting

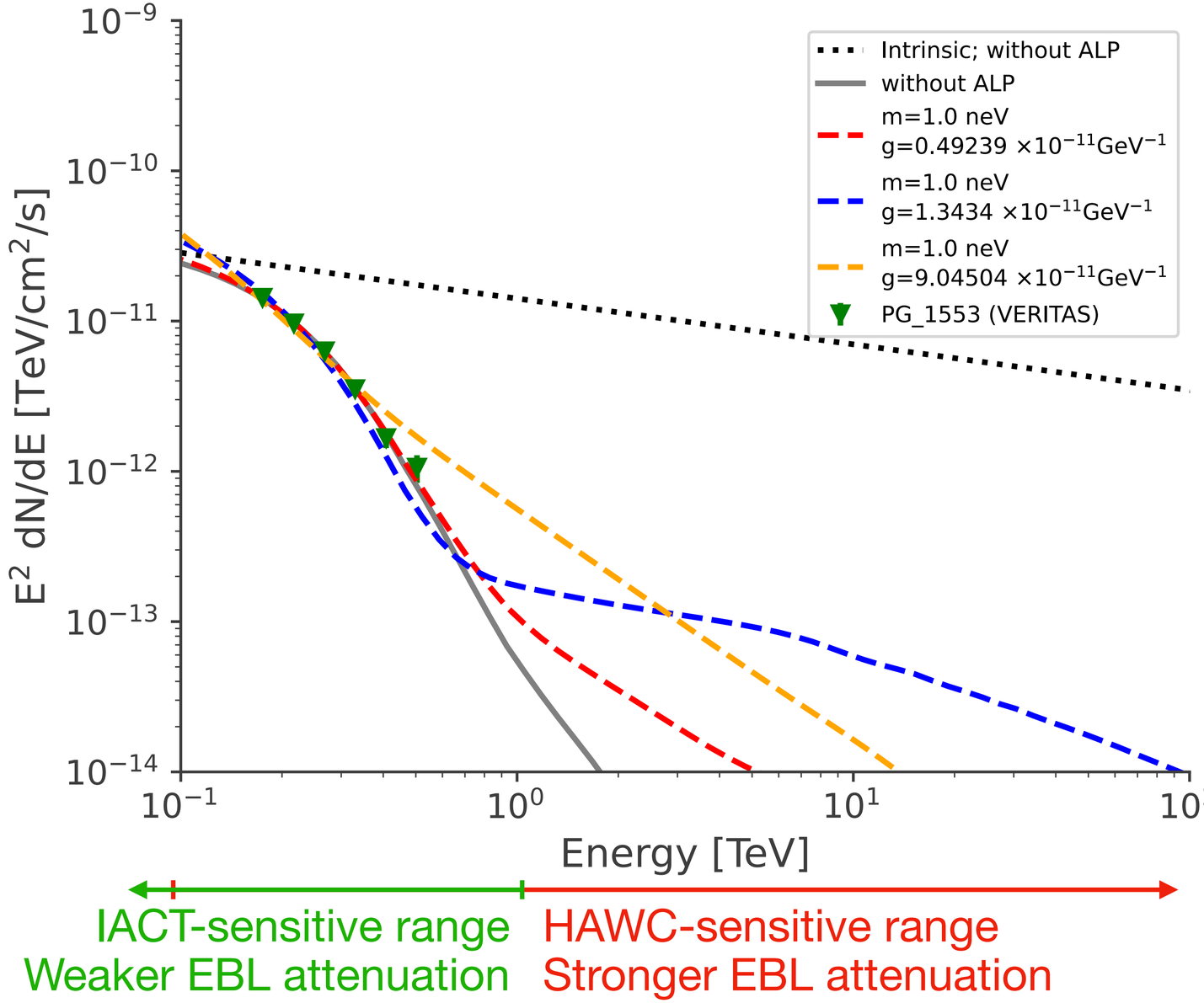

Intrinsic spectrum: $\Phi_\gamma^{\rm int} = K\left(\frac{E_\gamma}{1\ \rm TeV}\right)^{-\alpha}$

Observed spectrum: $\Phi_\gamma^{\rm obs} = \Phi_\gamma^{\rm int} \times P_\gamma$

Fit $\Phi_\gamma^{\rm obs}$ onto IACT and HAWC data!

(Maximize $\log L = \log L_{\rm IACT} + \log L_{\rm HAWC}$)

IACT observations will be used to fit the less-attenuated spectrum, allowing for an accurate determination of the intrinsic spectrum.

HAWC observations will be used to evaluate ALP effects.

$\rm LLR = 2 \times (\log L(0,\ 0) - \log L(m_a, g_{a\gamma}))$

LLR reflects how much the w/o ALP scenario describes data better than the w/ ALP scenario.

Combined Limits & Comparison

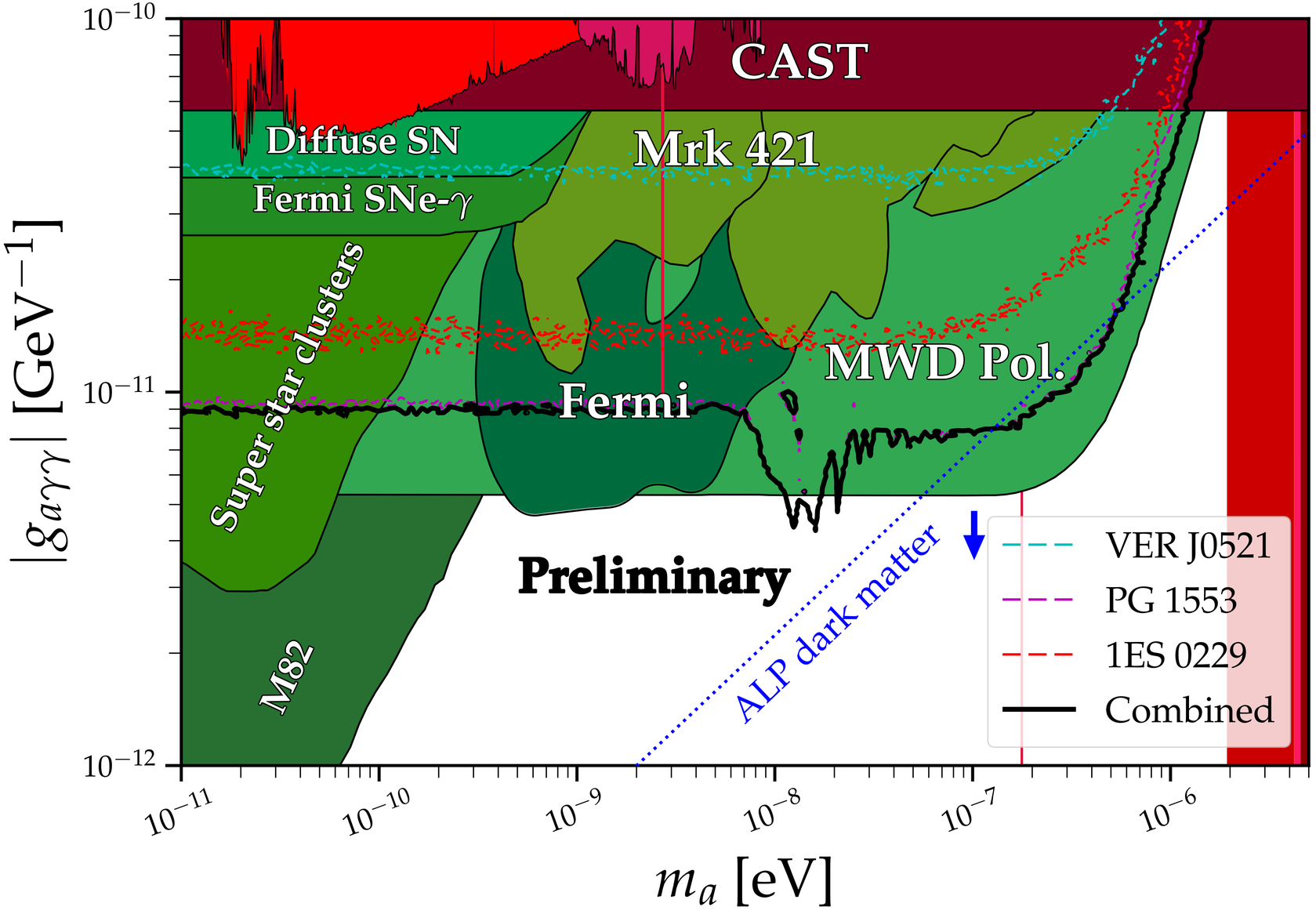

Backup

Event Binning

The events are binned based on the number of hits, core positions, and estimated energies.

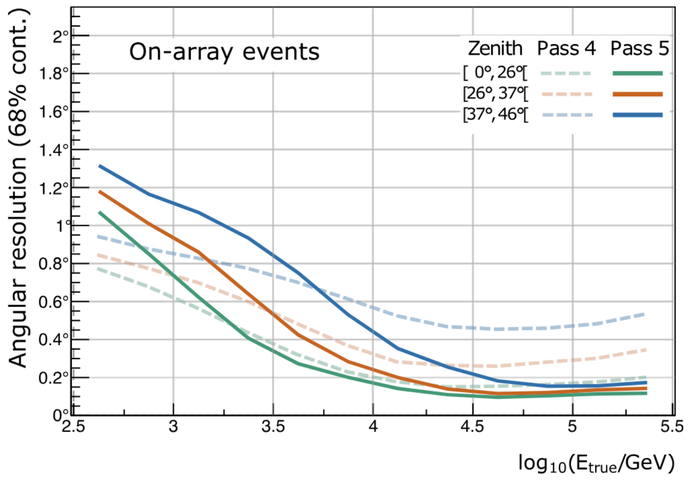

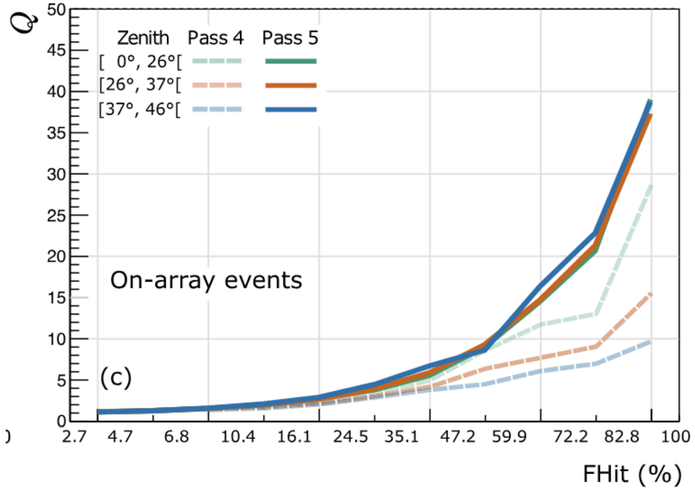

Pass 5	Hit PMT Fraction	Median Energy Crab On-array (TeV)	Median Energy Crab Off-array (TeV)
B0	2.7%–4.7%	0.28	0.57
B1	4.7%–6.8%	0.38	0.88
B2	6.8%–10.4%	0.53	1.29
B3	10.4%–16.1%	0.83	2.02
B4	16.1%–24.5%	1.37	3.66
B5	24.5%–35.1%	2.25	6.21
B6	35.1%–47.2%	3.68	10.27
B7	47.2%–59.9%	5.97	16.62
B8	59.9%–72.2%	9.54	25.78
B9	72.2%–82.2%	14.63	41.47
B10	82.2%–100.0%	30.46	73.91

Energy Bins	Min. $\log_{10}(E/\mathrm{GeV})$	Max. $\log_{10}(E/\mathrm{GeV})$
Ea	2.50	2.75
Eb	2.75	3.00
Ec	3.00	3.25
Ed	3.25	3.50
Ee	3.50	3.75
Ef	3.75	4.00
Eg	4.00	4.25
Eh	4.25	4.50
Ei	4.50	4.75
Ej	4.75	5.00
Ek	5.00	5.25
El	5.25	5.50

Statistical Framework

- HAWC usually uses maximum likelihood estimation to model the observations.
- Poisson distribution for the i-th “pixel” on the sky: $p_i = \dfrac{\theta_i^{n_i} e^{-\theta_i}}{n_i!}$,
  - where n_i is the number of events in pixel I and θ_i is the expected counts by the model.
- Then the log-likelihood is $\log L = \log\left(\prod_i^N p_i\right) = \sum_i^N \log p_i$.
- The test statistic (TS) is $\mathrm{TS} = 2\ln\left(L_{\mathrm{alt}}/L_{\mathrm{null}}\right)$, connected to $\sqrt{\mathrm{TS}} \sim$ Significance with the degree of freedom of one.

Transportation of particles

$$\frac{\partial N}{\partial t}(E,t) + \frac{\partial}{\partial E}\left[b(E)N(E,t)\right] + \frac{N(E,t)}{\tau_{esc}(E,t)} = Q(E,t)$$

$N(E,t)$: Electron spectrum

$b(E) = -\frac{dN}{dt}$: Loss rate by cooling (ICS, synchrotron, etc.) <- Given by photon production mechanism

$\tau_{esc}(E,t)$: escape time from the system

$Q(E,t)$: Injection spectrum <- Will be fitted

Pulsar basics

PSR

(Canonical pulsar assumption: $I = 10^{45}\ \mathrm{g\ cm^2}$)

Assume it is a rigid body (well, a pulsar is almost rigid). $E = \frac{I\Omega^2}{2} = \frac{2\pi^2 I}{P^2}$.

The derivative is $\dot{E} = I\Omega\dot{\Omega} = -\frac{4\pi^2 I\dot{P}}{P^3}$. -> A pulsar is losing energy by spinning down.

For a pulsar, P and $\dot{P}$ can be measured.

PSR J1849-0001: $P = 38.5\ \mathrm{ms},\ \dot{P} = 1.4156 \times 10^{-14}\ \mathrm{s/s}$ -> $\dot{E} = 9.6 \times 10^{36}\ \mathrm{erg/s}$

Assume the rotational energy ($\dot{E}$) is emitted through magnetic dipole radiation ($P = \frac{2}{3c^3}\dot{m}^2$) -> $\Omega \propto -\dot{\Omega}^3$

-> We know how the spin evolves ($\Omega \propto -\dot{\Omega}^3$), therefore, we can write $P(t)$, $\dot{E}(t)$, and $B(t)$.

Pulsar basics

(Canonical pulsar assumption: $I = 10^{45}\ \mathrm{g\ cm^2}$)

Assume it is a rigid body (well, a pulsar is almost rigid). $E = \frac{I\Omega^2}{2} = \frac{2\pi^2 I}{P^2}$.

The derivative is $\dot{E} = I\Omega\dot{\Omega} = -\frac{4\pi^2 I\dot{P}}{P^3}$. -> A pulsar is losing energy by spinning down.

For a pulsar, P and $\dot{P}$ can be measured.

PSR J1849-0001: $P = 38.5\ \mathrm{ms},\ \dot{P} = 1.4156 \times 10^{-14}\ \mathrm{s/s}$ -> Current $\dot{E} = 9.6 \times 10^{36}\ \mathrm{erg/s}$

Assume the rotational energy ($\dot{E}$) is emitted through magnetic dipole radiation ($P = \frac{2}{3c^3}\ddot{m}^2$) -> $\Omega \propto -\dot{\Omega}^3$

(Dipole radiation power: $P = \frac{2}{3c^3}\ddot{m}^2$ -> rotating dipole -> $m(t) = m_0 \sin\alpha \cos(\Omega t)$ -> $\ddot{m} \propto \Omega^2$.

If the spin-down powers the dipole radiation -> $\dot{E} = I\Omega\dot{\Omega} - P \propto -\dot{\Omega}^4$ -> $\Omega \propto -\dot{\Omega}^3$.)

-> We know how the spin evolves ($\Omega \propto -\dot{\Omega}^3$), therefore, we can write $P(t)$, $\dot{E}(t)$, and $B(t)$.

PWN-powered Accelerator

PSR

Wind

Energies
&
Electrons

Accelerated
electrons

Photon Fields
Klein-Nishina Xsection

CMB (observation)

Inferred IR & starlight

TeV
gamma rays

Cooling

Magnetic Field
Synchrotron

Radio to X-ray

Energy loss by spinning down:
$\dot{E}(t) = E_0(1+\tau/\tau_0)^{-2}$
$\dot{E}(t)$ to acceleration efficiency: η
Acceleration power: $L(t) = \eta\dot{E}(t)$

Injected electron spectrum
$Q_e(E_e,t) \propto E_e^{-\alpha} \times \exp\left(-E_e/E_{\rm cutoff}\right)$

Magnetic Field:
$B(t) = B_0\left(1+\sqrt{\tau/\tau_0}\right)^{-1}$

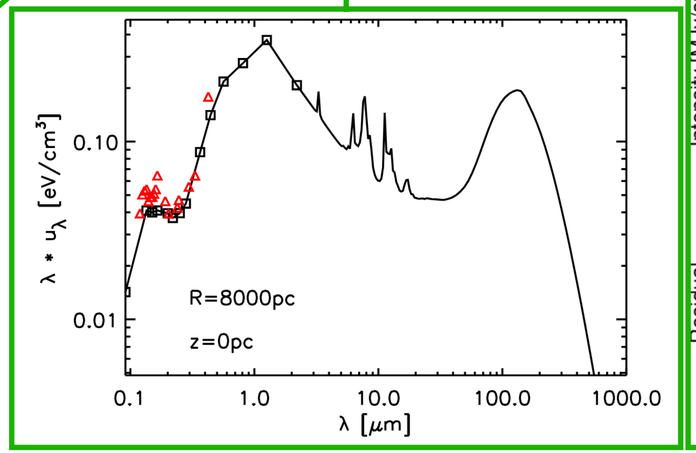

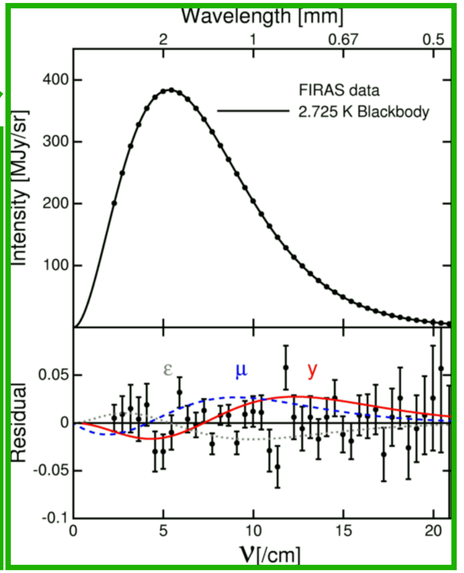

PWN-powered Accelerator

PSR

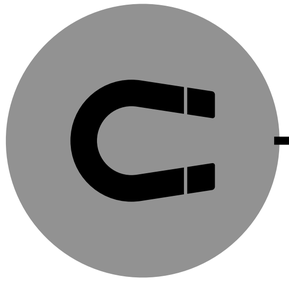

Energies
&
Electrons

Wind

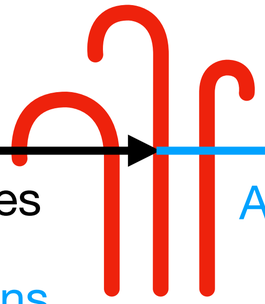

Accelerated electrons

Photon Fields

Klein-Nishina Xsection

CMB (observation)

Inferred IR & starlight

TeV
gamma rays

Magnetic Field
Synchrotron

Radio to X-ray

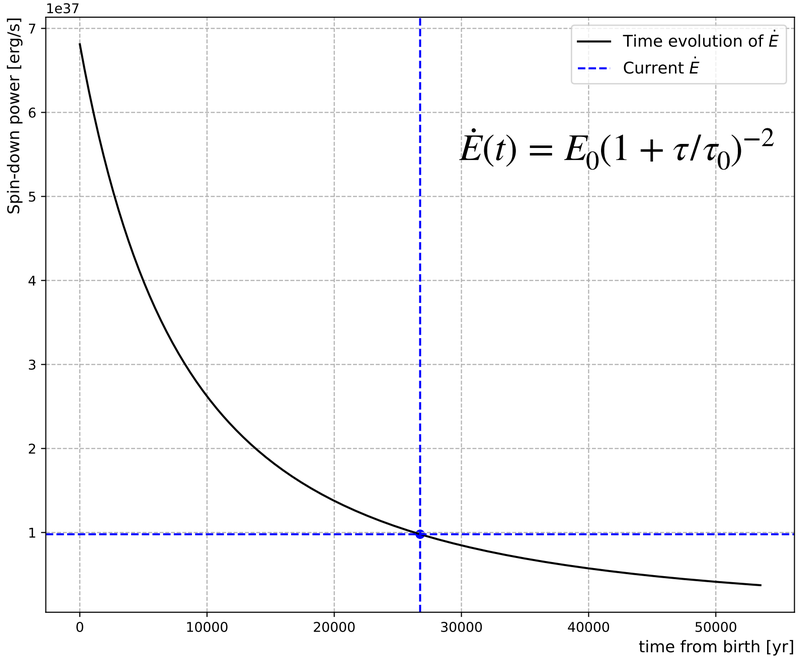

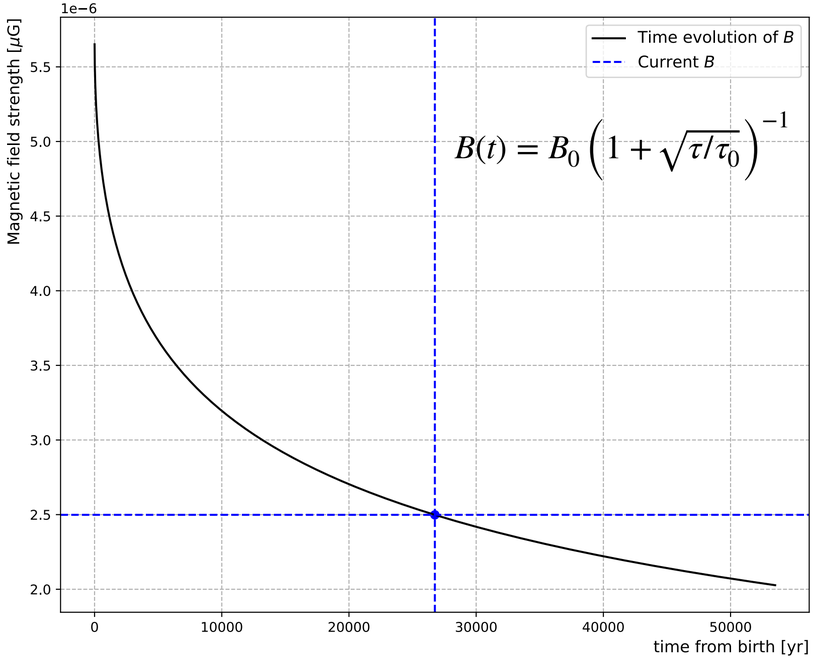

Fit Result

reported as (quantile $0.5\ ^{0.84}_{0.16}$)

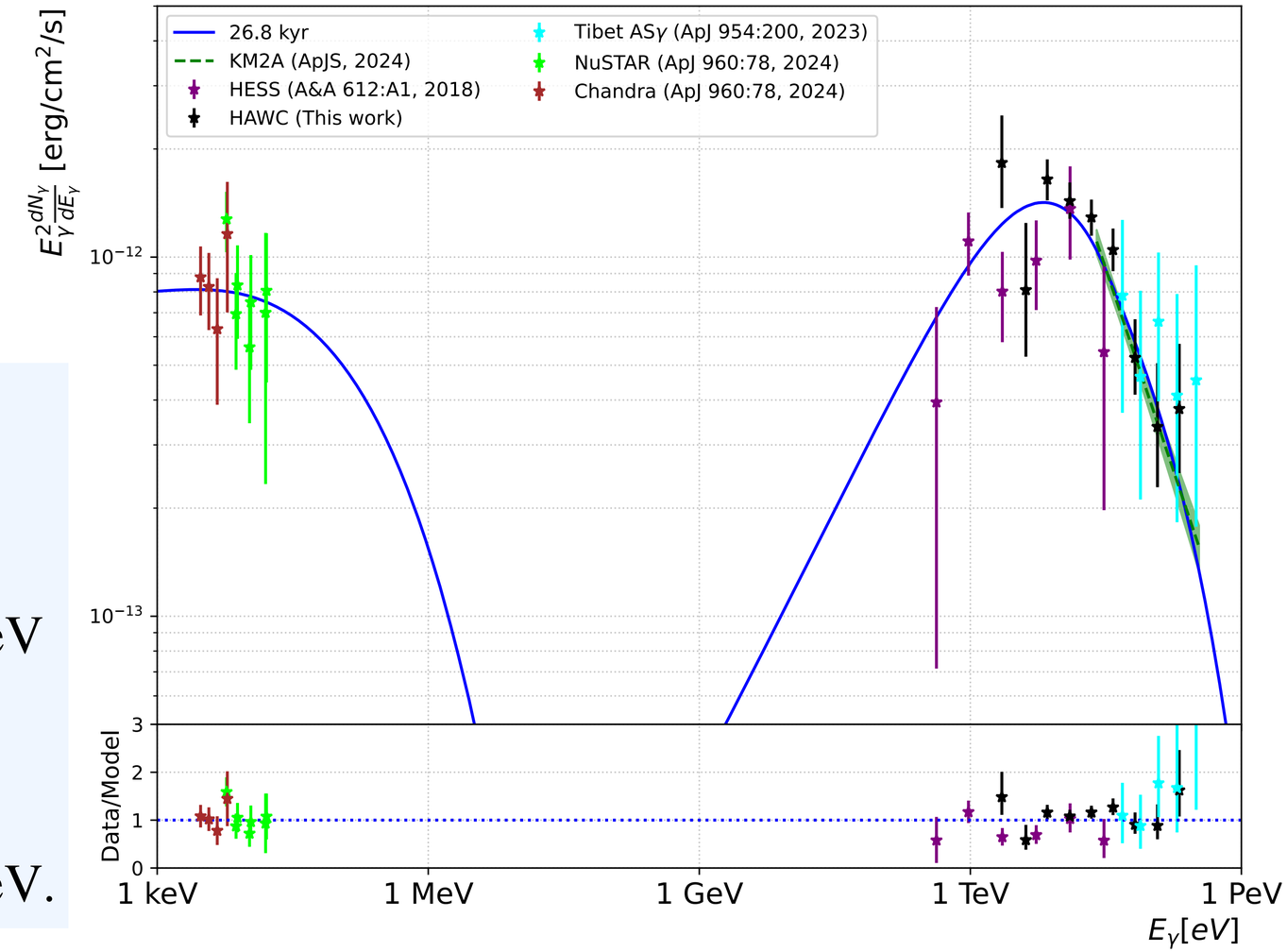

At Klein-Nishina regime (>100 TeV), ICS with CMB photons -> $E_e \simeq 2.15 \left(E_\gamma / 1\ \mathrm{PeV} \right)^{0.77}$.

At the electron cutoff energy $1.5^{+1.7}_{-0.6}$ PeV, $0.6^{+1.0}_{-0.3}$ PeV gamma can be produced.

From the LHAASO UHE source paper, the observed maximum photon energy is $E_{\gamma,\mathrm{max}} = 0.35 \pm 0.07$ PeV.

Backup for details

HAWC Event Classification

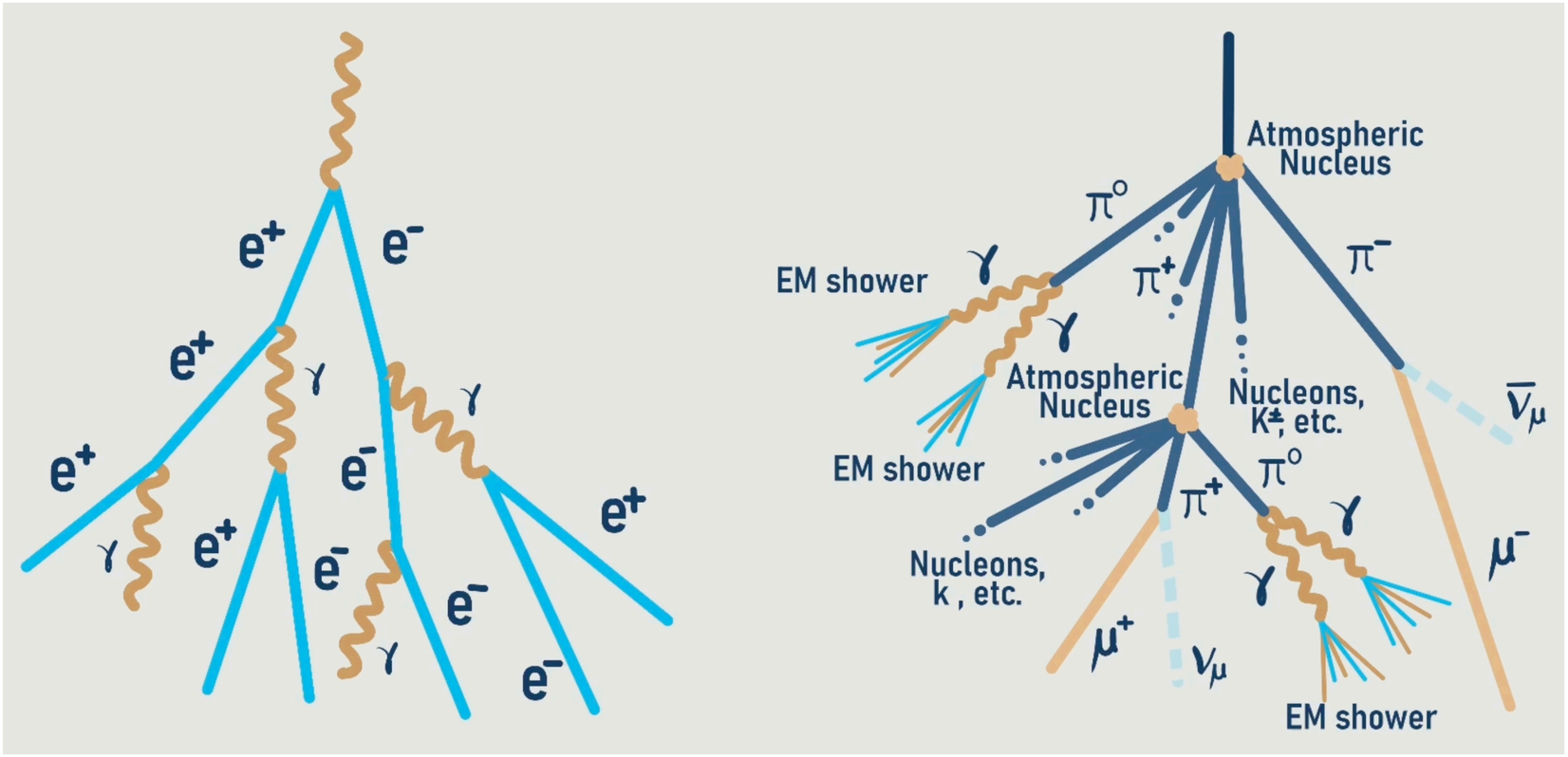

Rates: $\gamma : h \sim 1 : 1000$

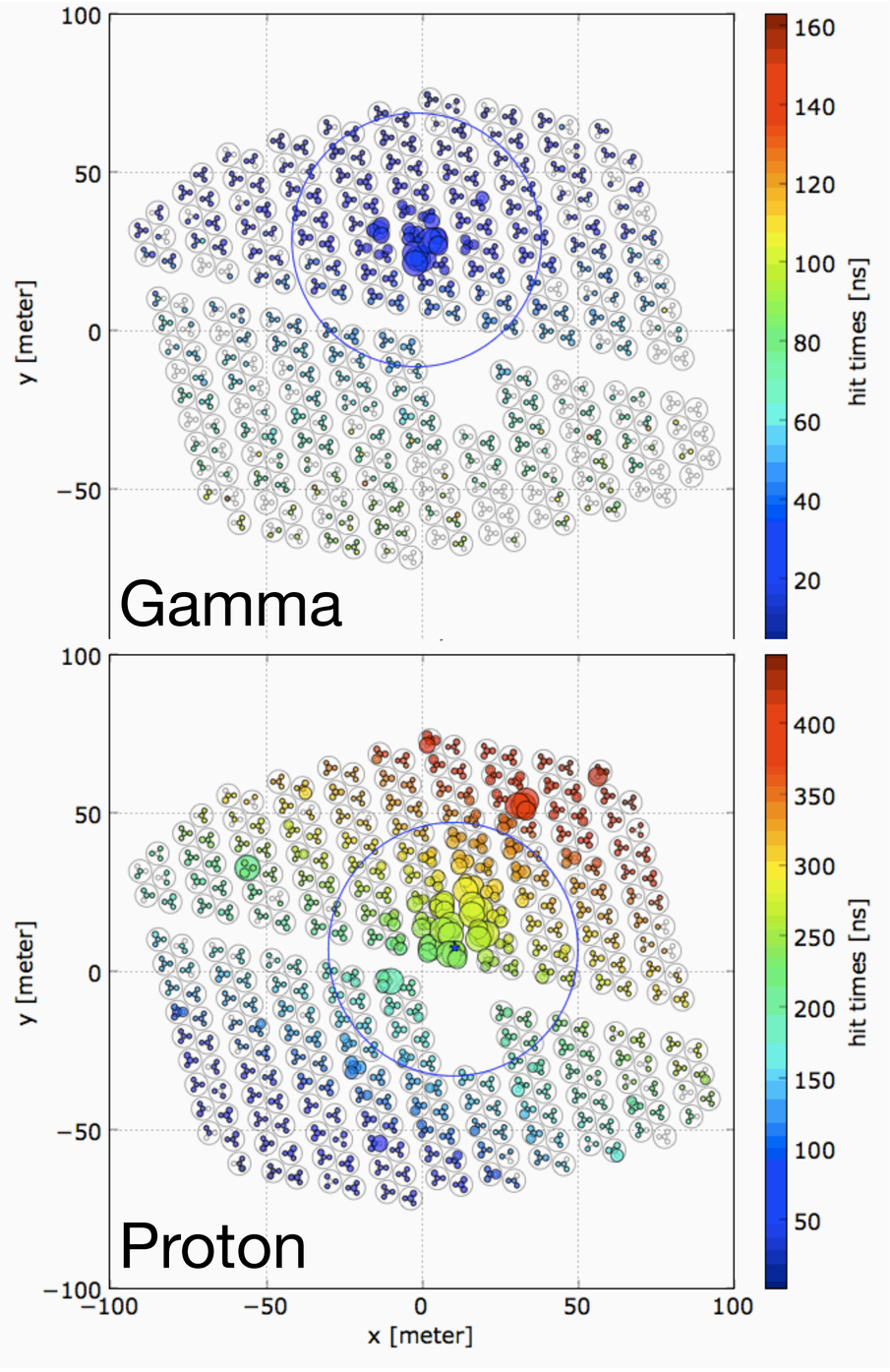

Event Classification

$$\mathrm{LIC} = \log_{10} \frac{\mathrm{CxPE}_{40\mathrm{m}}}{N_{\mathrm{hit}}}$$

$\mathrm{CxPE}_{40\mathrm{m}}$ is the largest effective charge far (>40 m) from the shower core.

-> Muons (rich in hadronic showers) cause large $\mathrm{CxPE}_{40\mathrm{m}}$.

-> High LIC for hadron-induced showers

LDFChi2 is the reduced χ^2 from the lateral distribution function (LDF) fit, describing how the number of particles or radiation varies with the distance from the shower core.

-> Gamma-induced showers are concentrated near the shower axis.

-> Low **LDFChi2** for gamma-induced showers

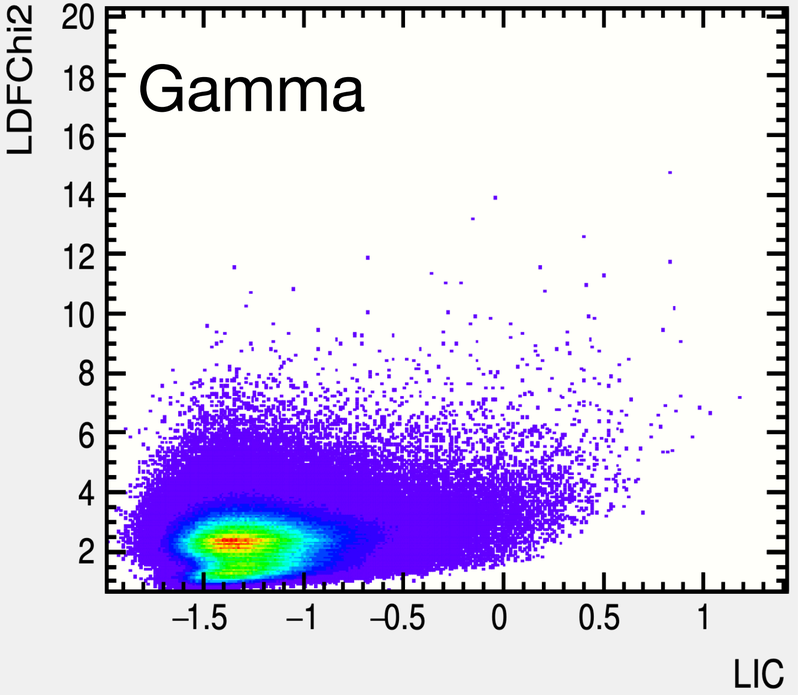

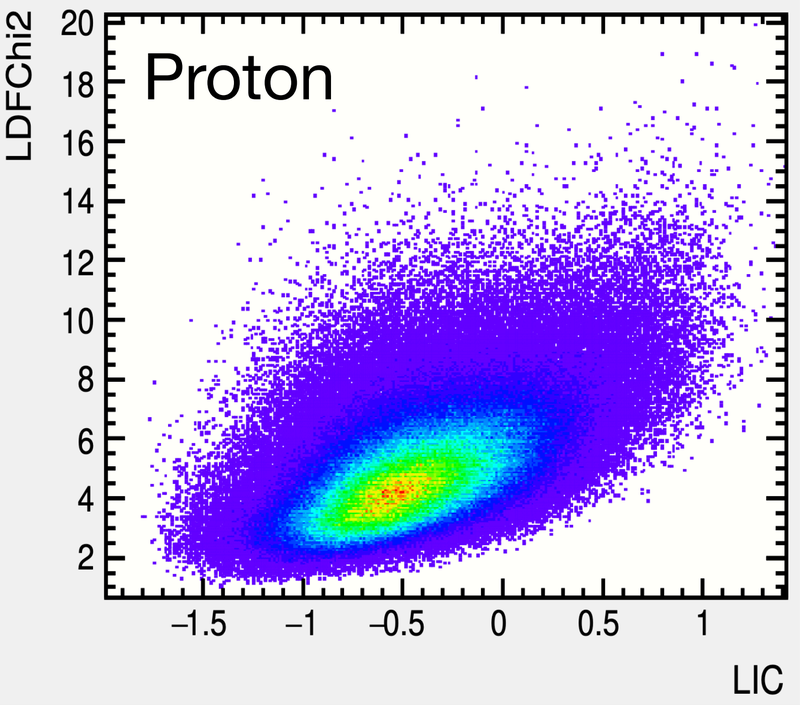

Event Reconstruction

Three main parameters are needed for the high-level analysis:

* Core: Center of the shower -> This affects the reconstruction performance; therefore, it is a main binning variable.

* Primary direction: The directional vector is fitted by minimizing

$$\chi^2 = \sum_{n=1}^{N} w_n \left(ct_n - ct_0 + \vec{i}x_n + \vec{j}y_n + \vec{k}z_n \right)^2 .$$

For n-th PMT, $c(t_n - t_0)$ is the relative trigger time,
w_n is the weight (inverse log-charge),
$(x_n,\ y_n,\ z_n)$ is the PMT position.

$$(\vec{r} = \cos\theta \sin\phi \vec{i} + \sin\theta \sin\phi \vec{j} + \cos\theta \vec{k})$$

* Primary energy: GP (from shower function fitting) and NN (neural net)

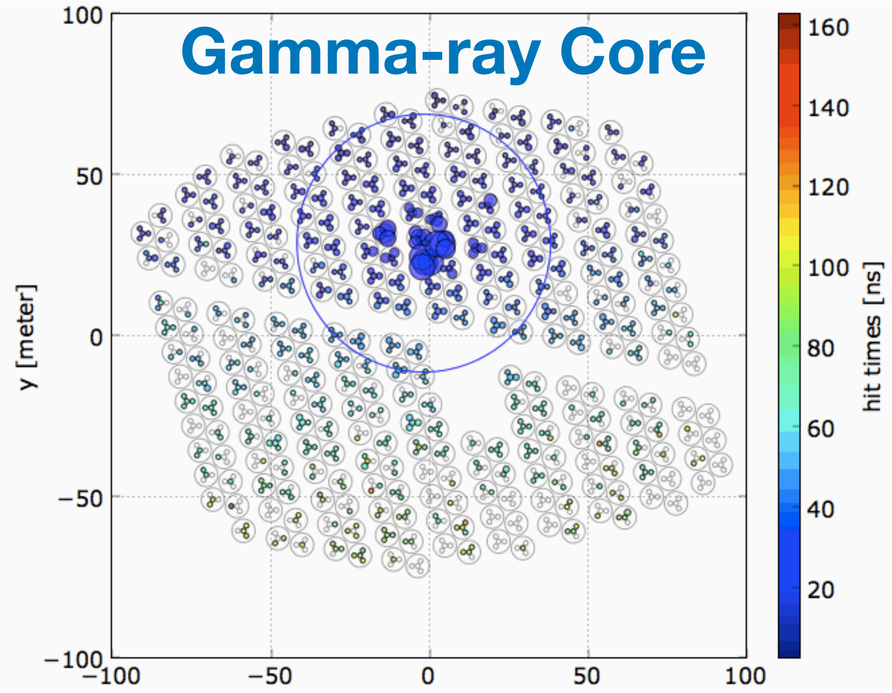

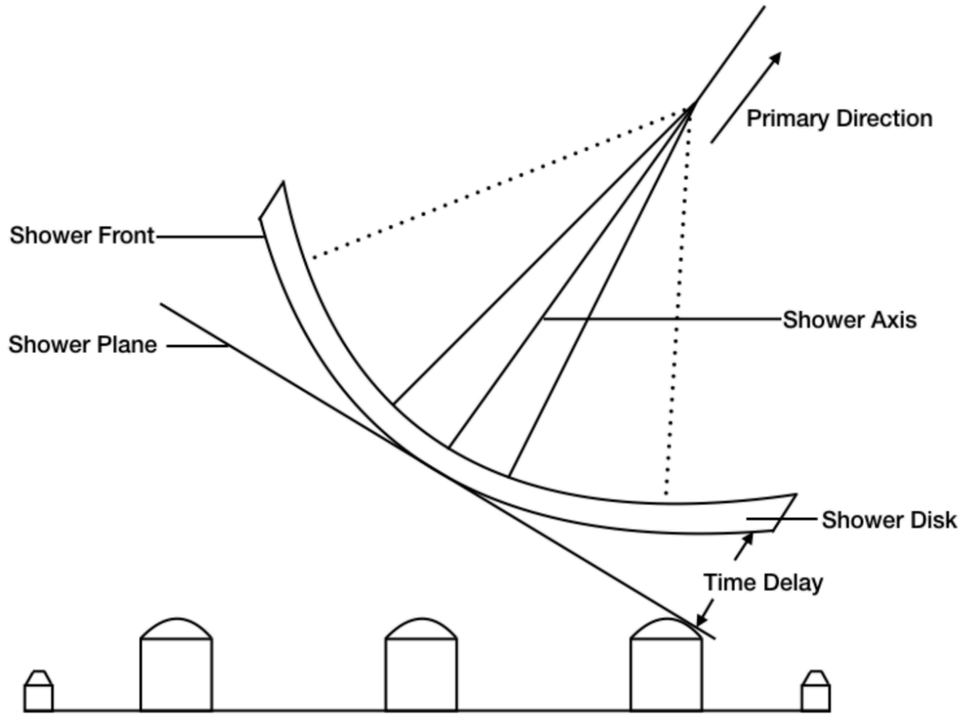

Cherenkov Radiation

A charged particle emits Cherenkov radiation when it travels faster than the speed of light in a medium (water).

$\cos(\theta_C) = \frac{c}{nv}$ -> θ_C is Cherenkov angle.

-> Cherenkov angle in water -> 41 degrees (n=1.33 where v~c)

EAS

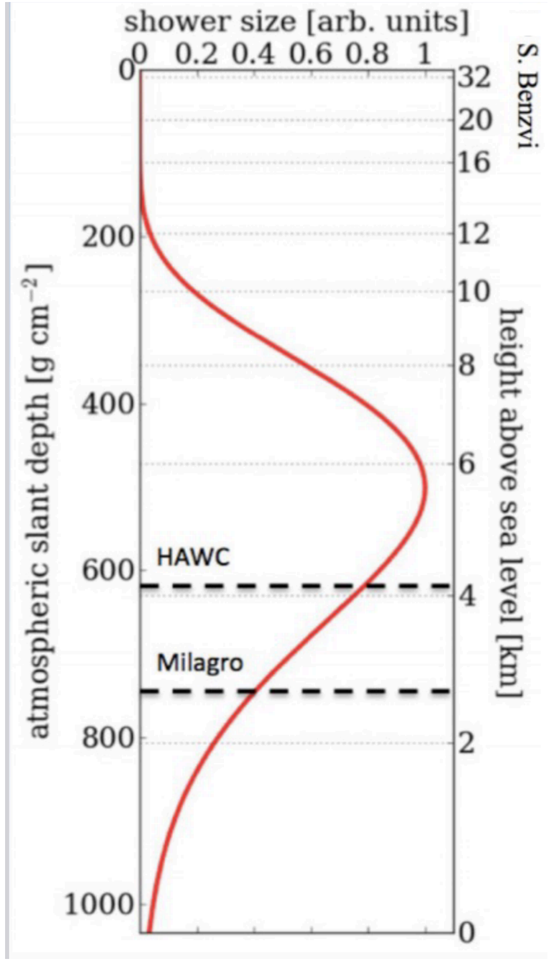
shower size [arb. units]
0 0.2 0.4 0.6 0.8 1
S. Benzvi
atmospheric slant depth [g cm^{-2}]
height above sea level [km]
0
200
400
600
800
1000
32
20
16
12
10
8
6
4
2
0
HAWC
Milagro

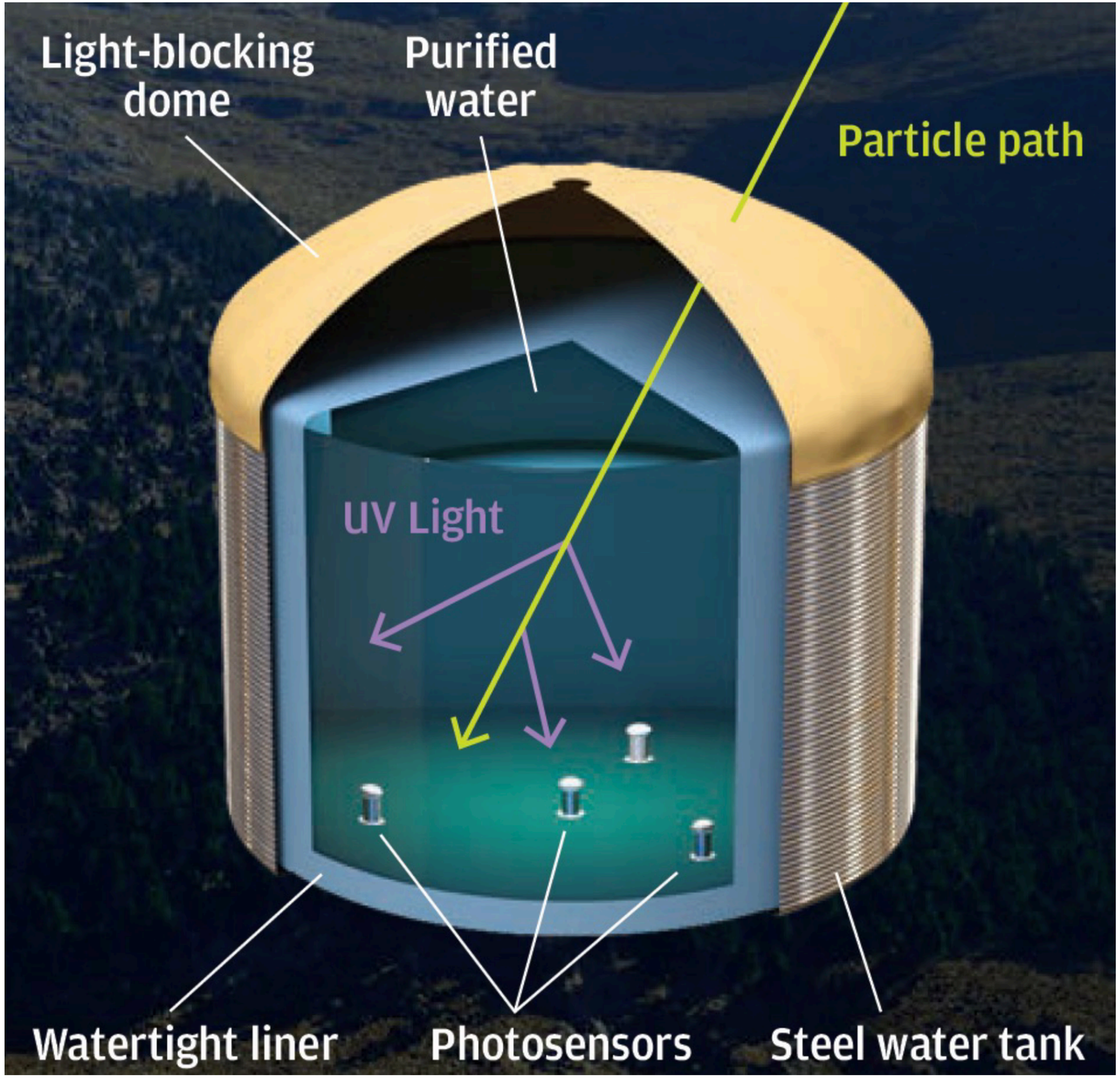
Light-blocking dome
Purified water
Particle path
UV Light
Watertight liner
Photosensors
Steel water tank

ALP

Interaction: $L_{a\gamma\gamma} = -\frac{1}{4} g_{a\gamma\gamma} F_{\mu\nu} \tilde{F^{\mu\nu}}$

Mixing eq. (Schrodinger-like) : $\left(i\frac{d}{dz} + E + \mathscr{M} \right) \Phi(z) = 0$

$$\mathcal{M} = \begin{pmatrix} \Delta_\perp & 0 & 0 \\ 0 & \Delta_{||} & \Delta_{a\gamma} \\ 0 & \Delta_{a\gamma} & \Delta_a \end{pmatrix}$$

The photon-ALP system propagates to the z-axis through a transverse B-field $B_\perp$,
with the state vector $\Phi = \left(A_x, A_y, a \right)^T$.

$T_i = \exp[-i(E + \mathscr{M})dz_i]$

Divide N path, calculate transfer matrix, $\mathscr{T} = \prod_{i=1}^{N} \mathscr{T}_i$ –> density matrix: $\rho(z) = \mathscr{T} \rho(0) \mathscr{T}^\dagger$

$P_\gamma = \mathrm{Tr}[(\rho_{11} + \rho_{22})\rho(z)]$

J1842 & SS 433 Analysis

This dissertation contains two additional analyses on the galactic sources: J1842 and SS 433.

Both analyses were published:

* *HAWC Study of the Very-high-energy γ-Ray Spectrum of HAWC J1844−034 (ApJ 2023)*
* *Spectral Study of Very-high-energy Gamma Rays from SS 433 with HAWC (ApJ 2024)*

The dissertation contains four analyses, so I cannot go through all the details as I did for J1850 analysis.

I will skip the details of HAWC data analysis and instead highlight the key scientific results.

(The details are similar to J1850:
Pass5 Improvement, blind source search)

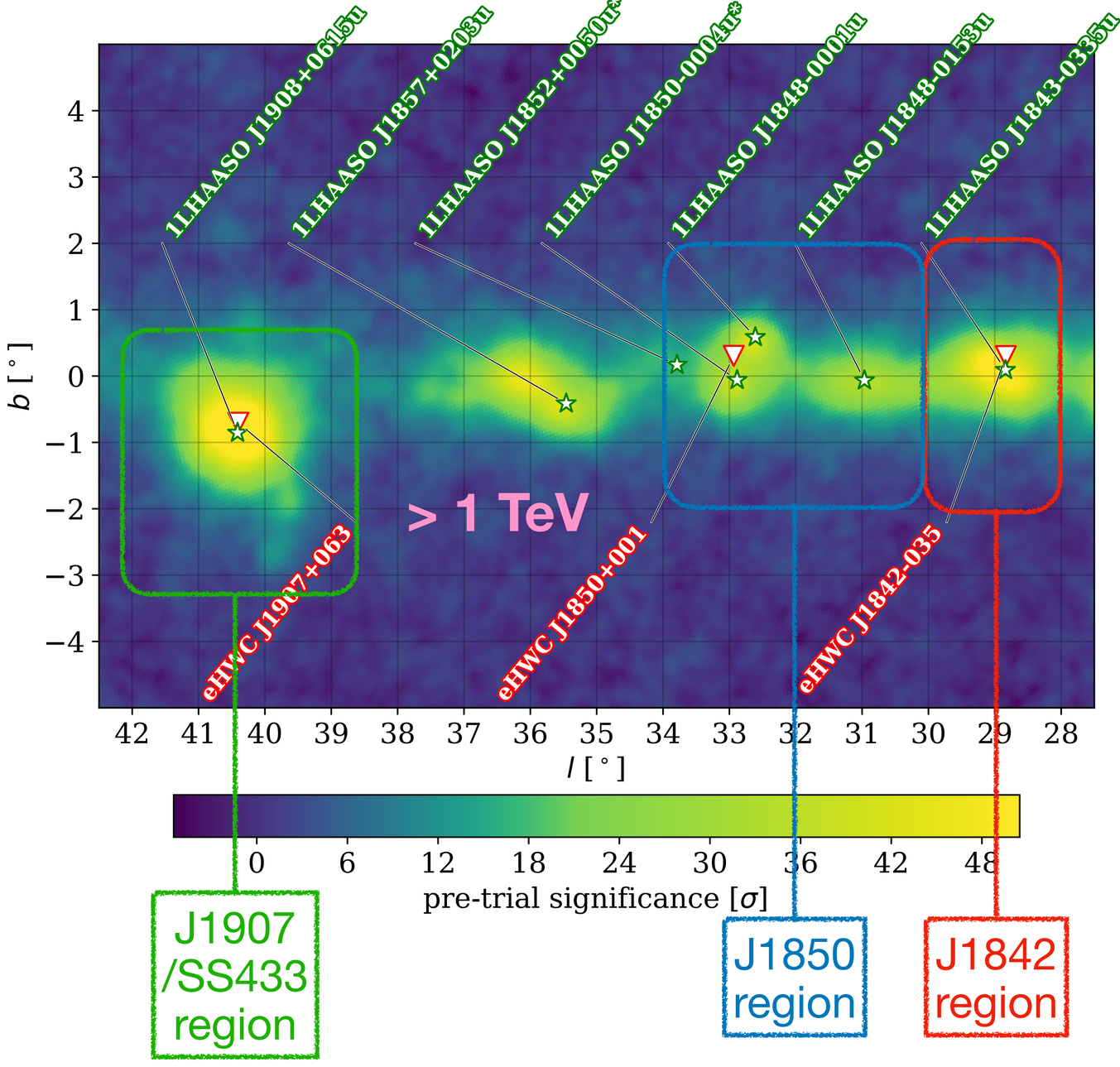

SNR G28.6-0.1

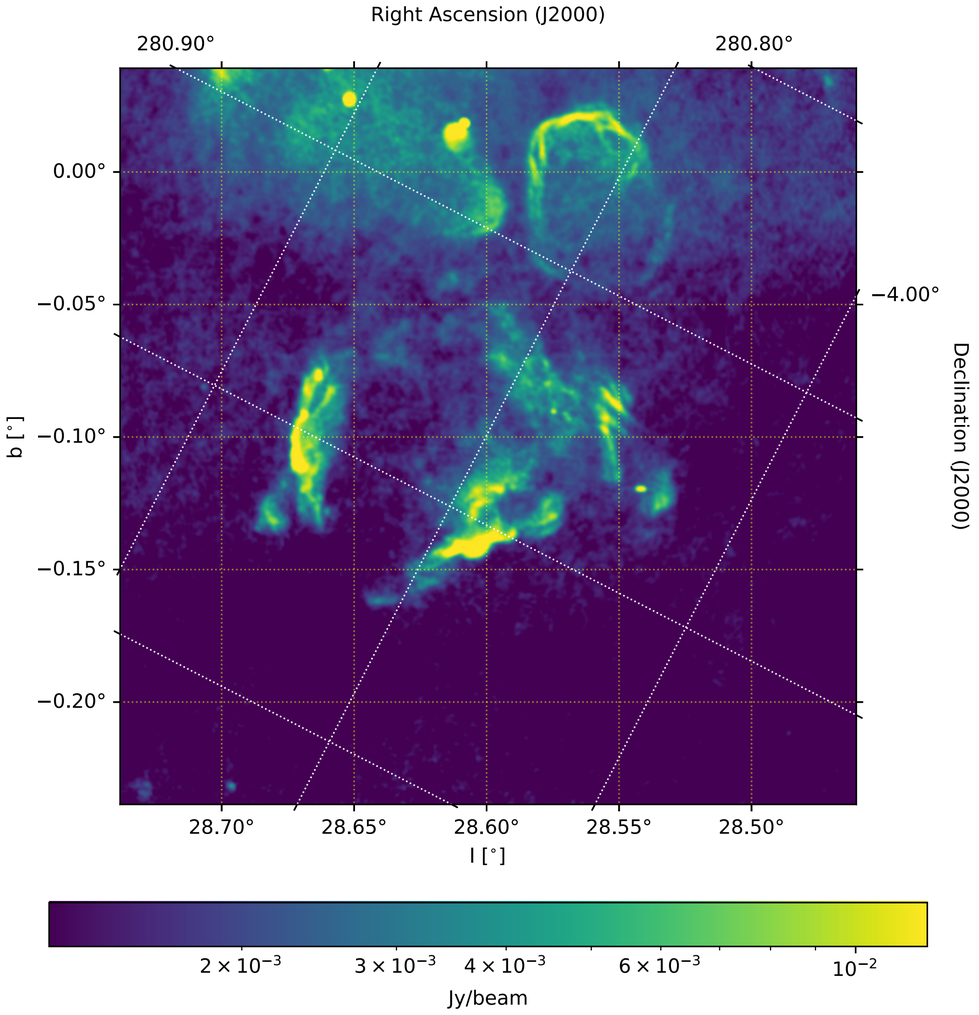

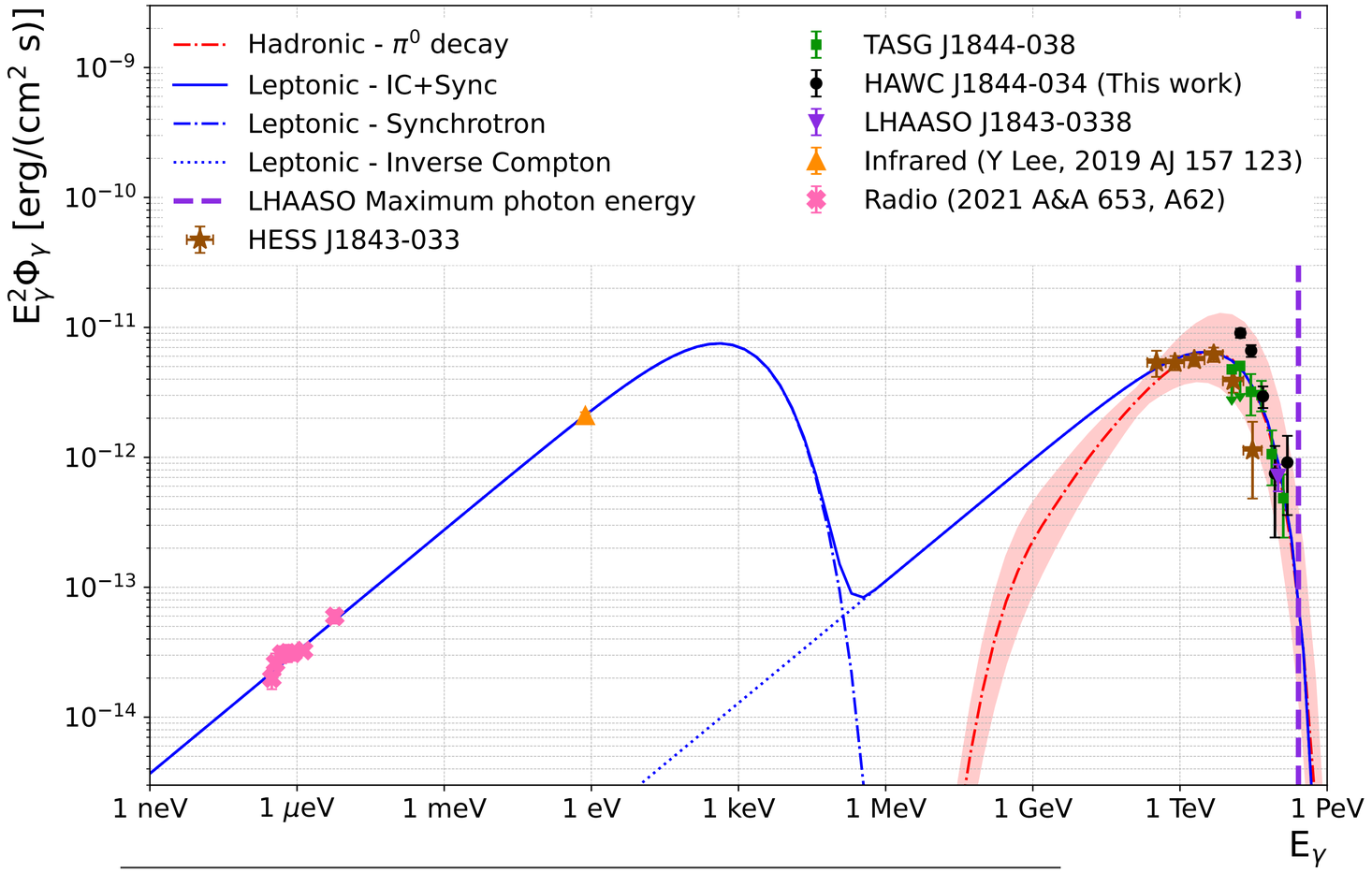

$\Phi_{0,e(9.6\mathrm{kpc})}$ [1/eV]	Γ_e	$E_{\mathrm{cutoff},e}$ [TeV]	B [μG]
$8.03^{+0.54}_{-0.52} \times 10^{33}$	$2.37^{+0.01}_{-0.01}$	$92.2^{+6.2}_{-6.7}$	$2.85^{+0.17}_{-0.16}$

SNR G28.6-0.1 has been observed in radio and infrared. -> Fitting synchrotron emissions is possible!

A single electron population can explain the observations from low-energy to multi-TeV, with a reasonable B-field.

SS 433 Spectra

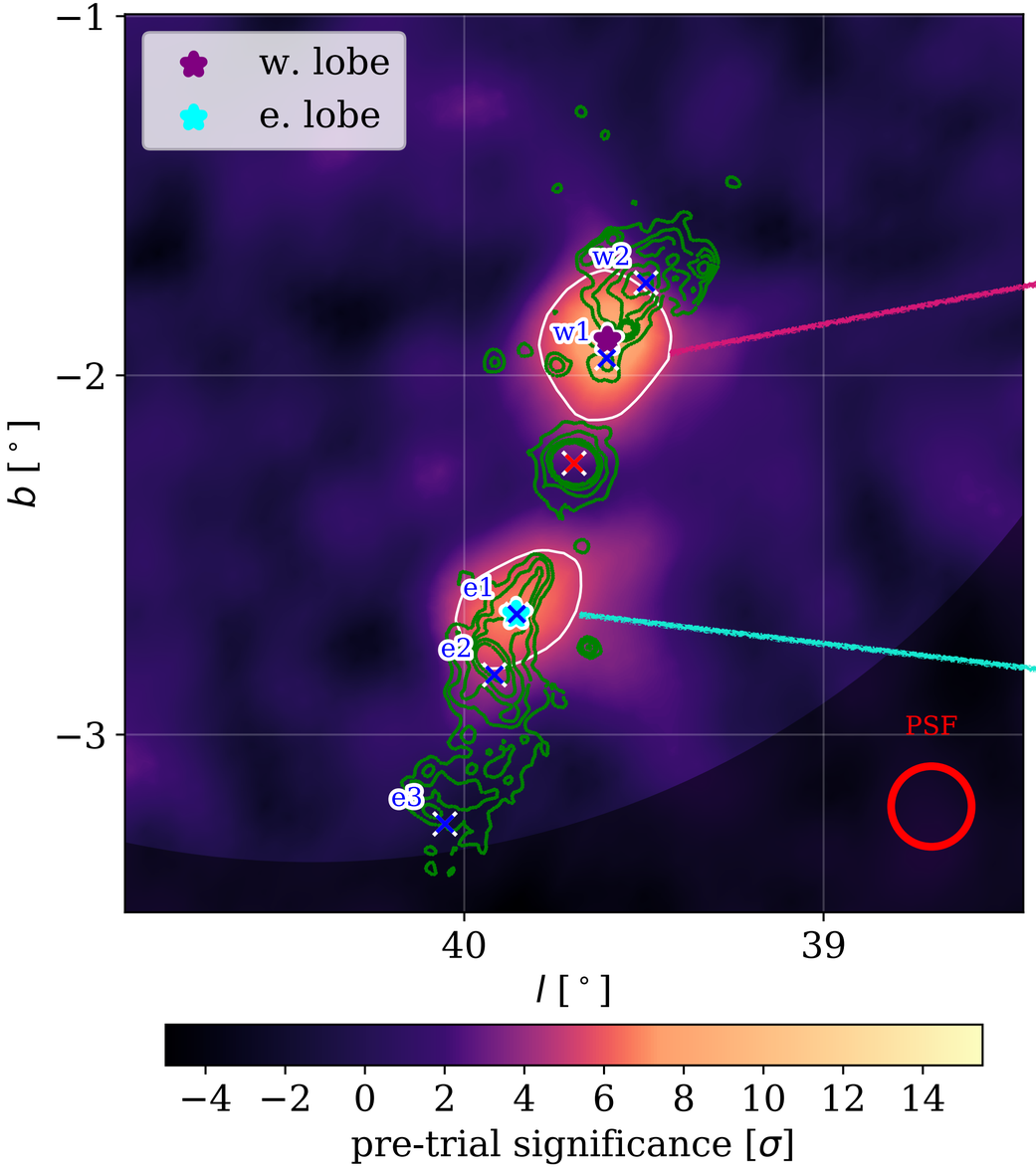

$$\Phi\left(E_\gamma\right) = \Phi_0 \left(\frac{E_\gamma}{E_0}\right)^{-\alpha}$$

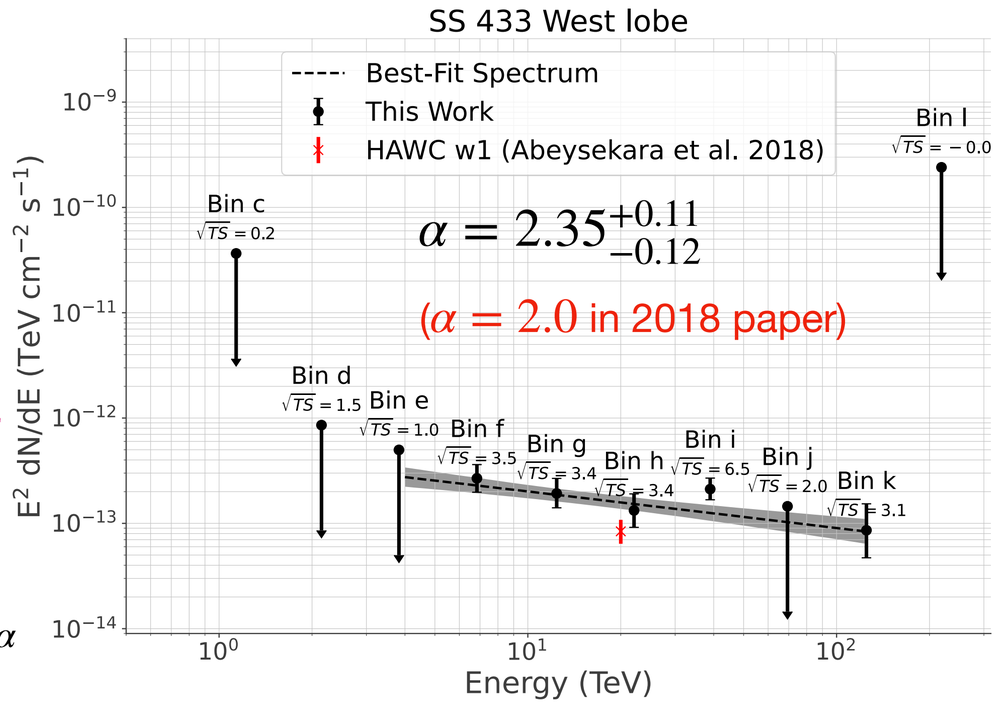

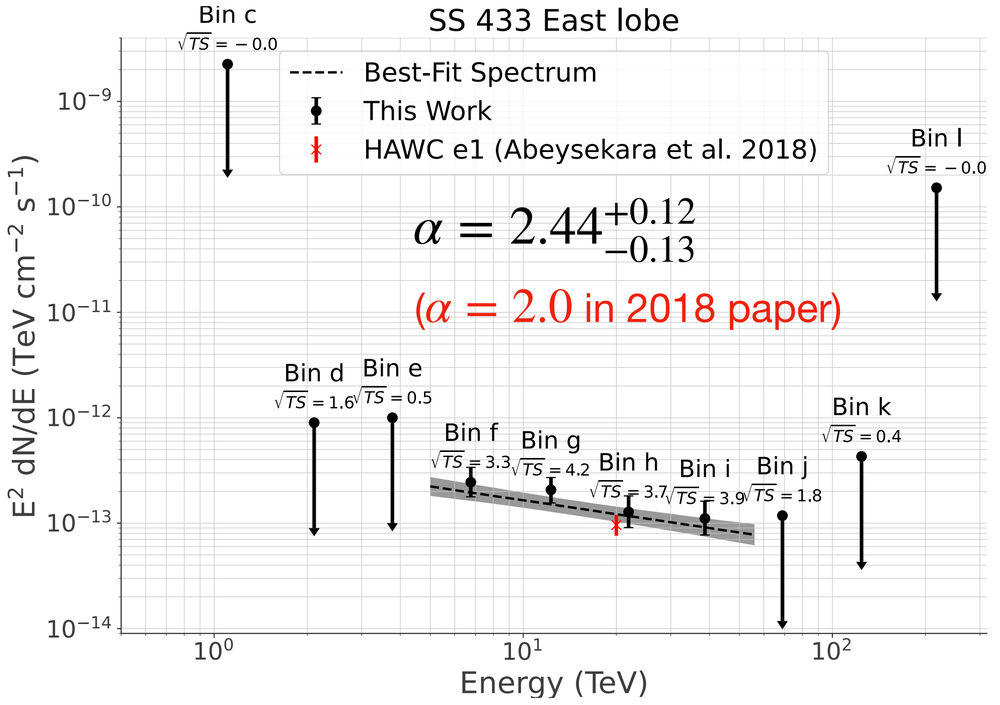

SS 433 Theoretical Modeling

Theoretical modeling was done by Prof. Ke Fang (one of the primary authors of this paper)

A steady one-zone electron injection model (same as the discovery paper)

-> The model found $W_e = 1.3 \times 10^{47}$ erg.
smaller than the kinetic power of the jets 9×10^{50} erg

-> The model is in tension at the west jet's multi-TeV range. It suggests that the photon production mechanism may be more complicated than a one-zone model (X-ray and gamma rays are from the same electron population).

(The hadronic model was already disfavored in the discovery paper since it requires extreme source parameters, 30% of kinetic power.)

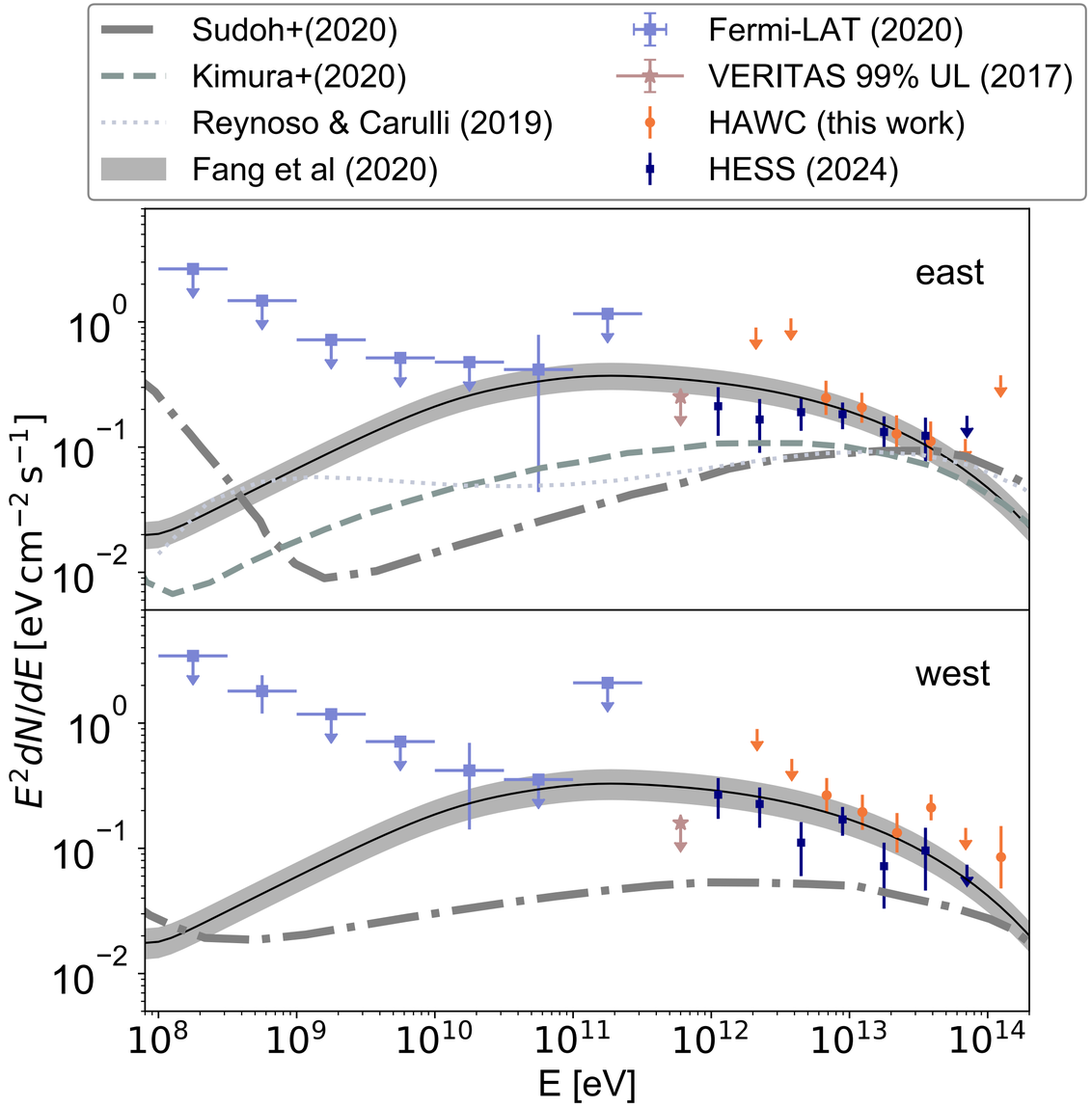

Blind Search Results

Three extended sources found. Each of them has a counterpart at different observatories' catalogs.

HAWC (This work, 1-316 TeV)	H.E.S.S. (2018, 0.3-30 TeV)	LHAASO KM2A (2024, 25-1000 TeV)
HAWC J1848-0145	HESS J1848-018	KM2A J1848-0153u
HAWC J1849-0000	HESS J1849-000	KM2A J1848-0001u
HAWC J1852-0002	HESS J1852-000	KM2A J1850-0004u*

Assumed spectrum: power-law
Assumed morphology: Gaussian
- HAWC J1848-0145 features an elliptical Gaussian.

Detailed searches in the spectrum and morphology are needed.
i.e.) Does the spectrum have a curvature or cutoff?

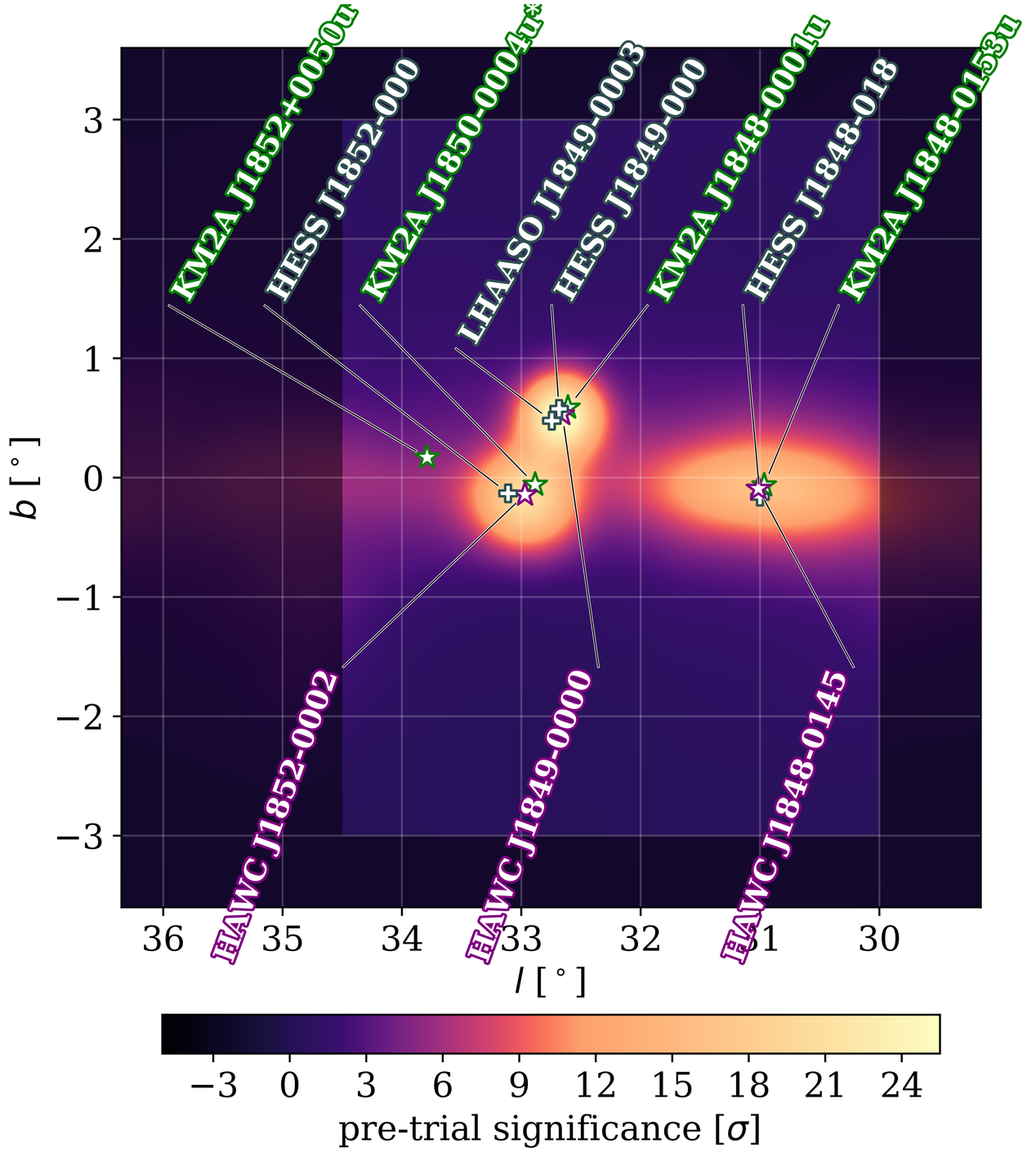

Detailed Component Modeling

Log parabola spectrum (LogP): $\Phi\left(E_\gamma\right) = \Phi_0\left(\frac{E_\gamma}{E_0}\right)^{-\alpha-\beta\log\left(E_\gamma/E_0\right)}$

Cutoff power-law spectrum (COPL): $\Phi\left(E_\gamma\right) = \Phi_0\left(\frac{E_\gamma}{E_0}\right)^{-\alpha}\exp\left(-\frac{E_\gamma}{E_{\text{cutoff}}}\right)$

Morphology: $\phi(\text{lon},\text{lat}) = \phi(r) = N\exp\left[-\left(\frac{r}{r_0}\right)^{1/\eta}\right]$

$N = \frac{1}{2\pi r_0^2\eta\Gamma(2\eta)}$

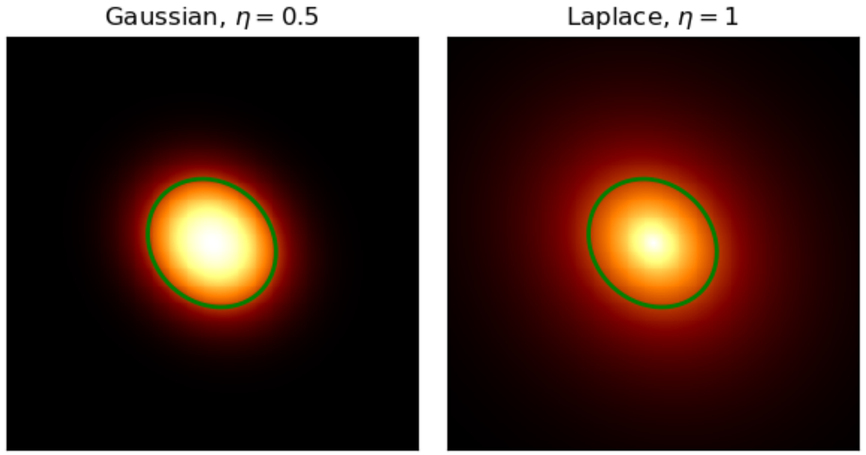

Source	Spectrum	Morphology	ΔTS
J1848	LogP	Asymmetric	32
J1848	**COPL**	**Asymmetric**	43
J1849	LogP	Gaussian	28
J1849	COPL	Gaussian	20
J1849	PL	Laplace	4
J1849	**LogP**	**Laplace**	36
J1849	COPL	Laplace	28
J1852	LogP	Gaussian	68
J1852	COPL	Gaussian	66
J1852	PL	Laplace	9
J1852	**LogP**	**Laplace**	85
J1852	COPL	Laplace	84

Modeling Results

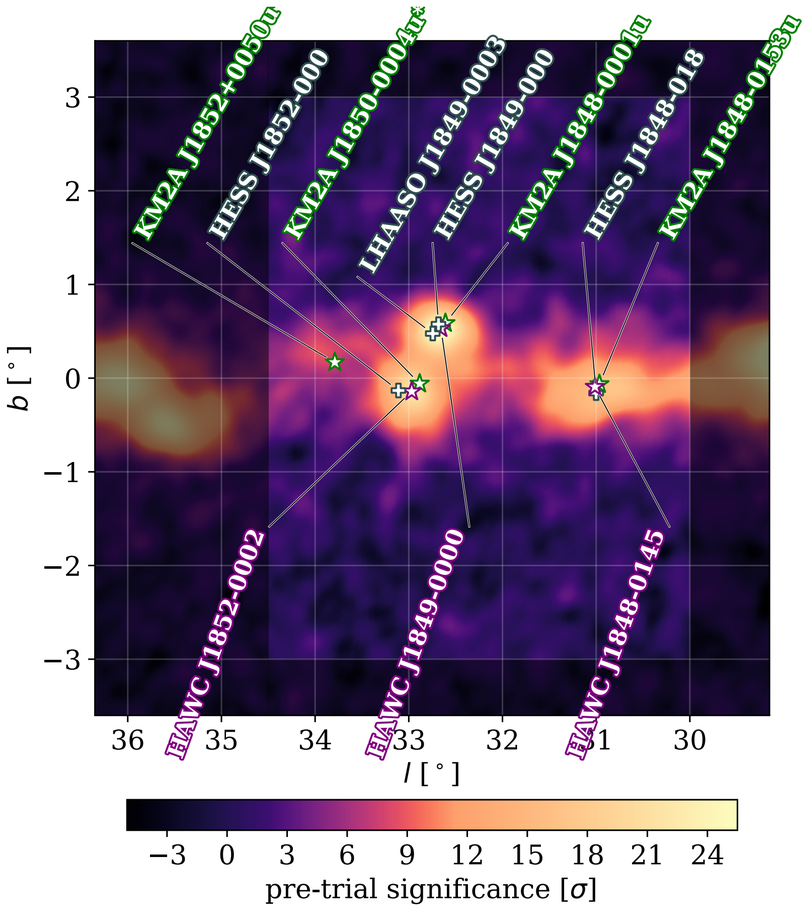

Data Map

−

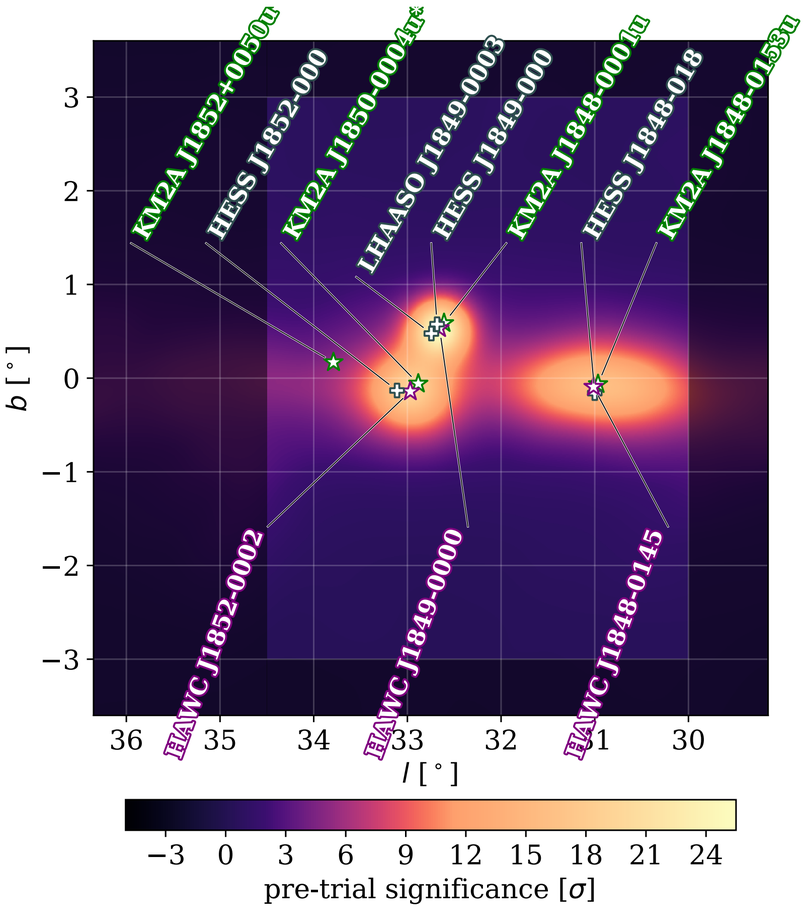

Model Map

=

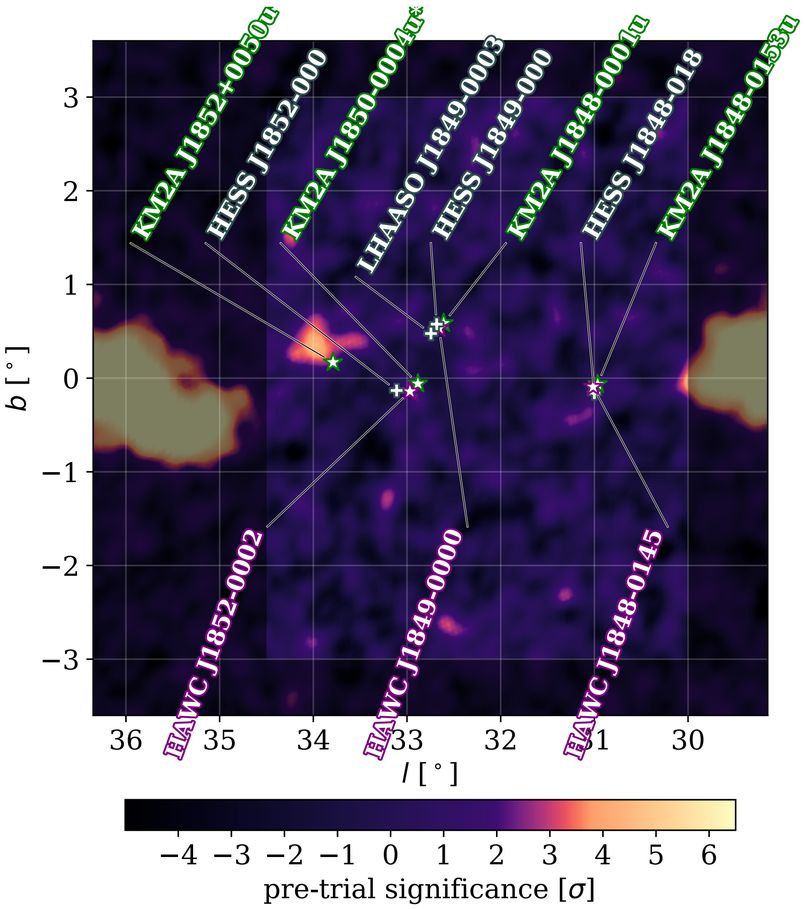

Residual Map

- A hotspot came out at $(l,\ b) \sim (34,\ 0.5)$ after the detailed modeling.
- Need to be cleaned up.

LLR-based Limits

$$\mathrm{LLR} = 2(\log L(0,\ 0) - \log L(m_a, g_{a\gamma}))$$

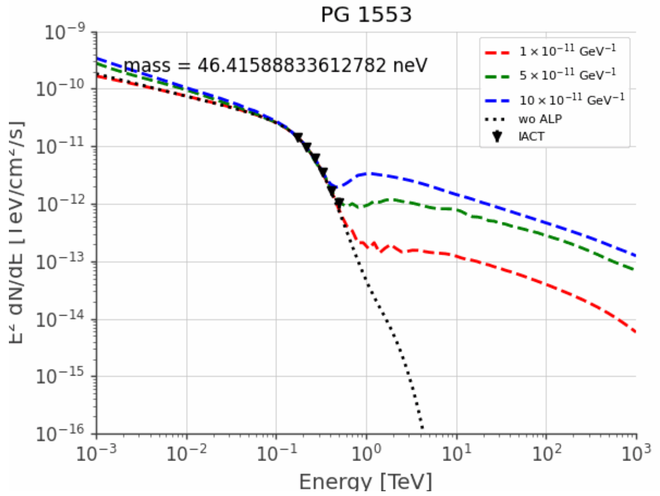

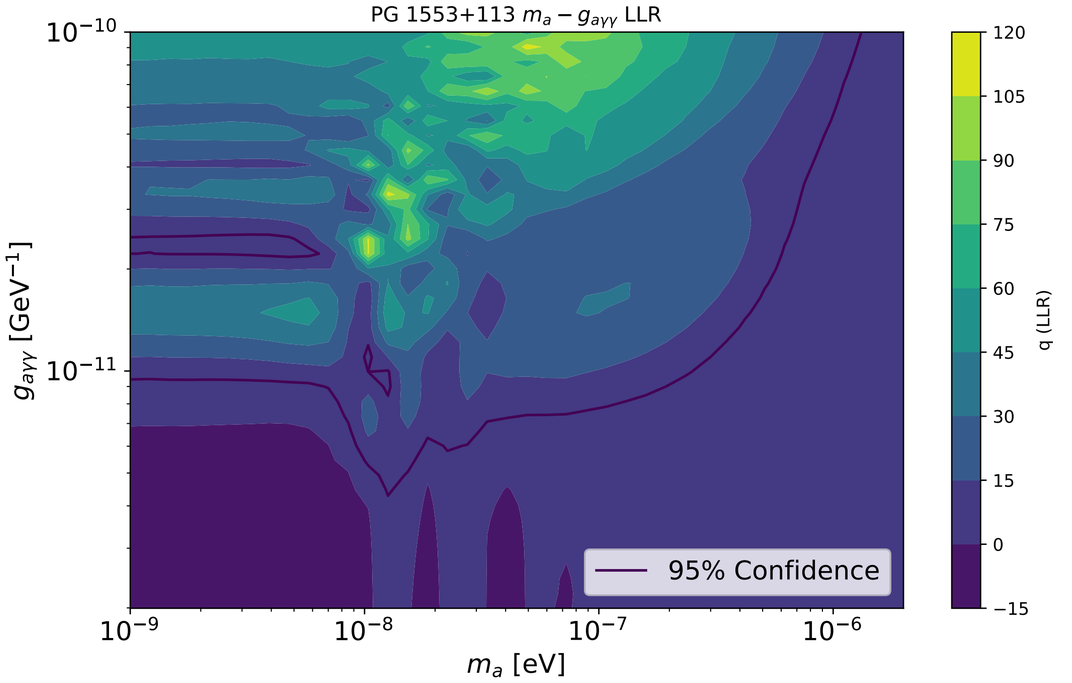

High LLR -> Null hypothesis is more likely.

Degrees of freedom of two -> $\chi^2 > 5.99$ for 95% CL exclusion

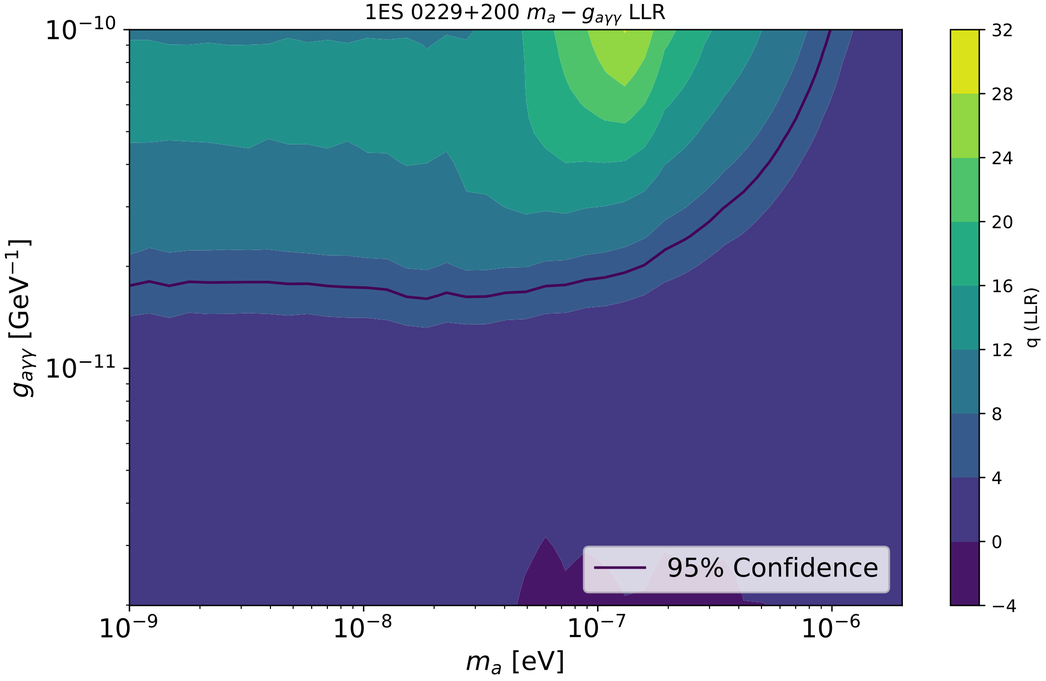

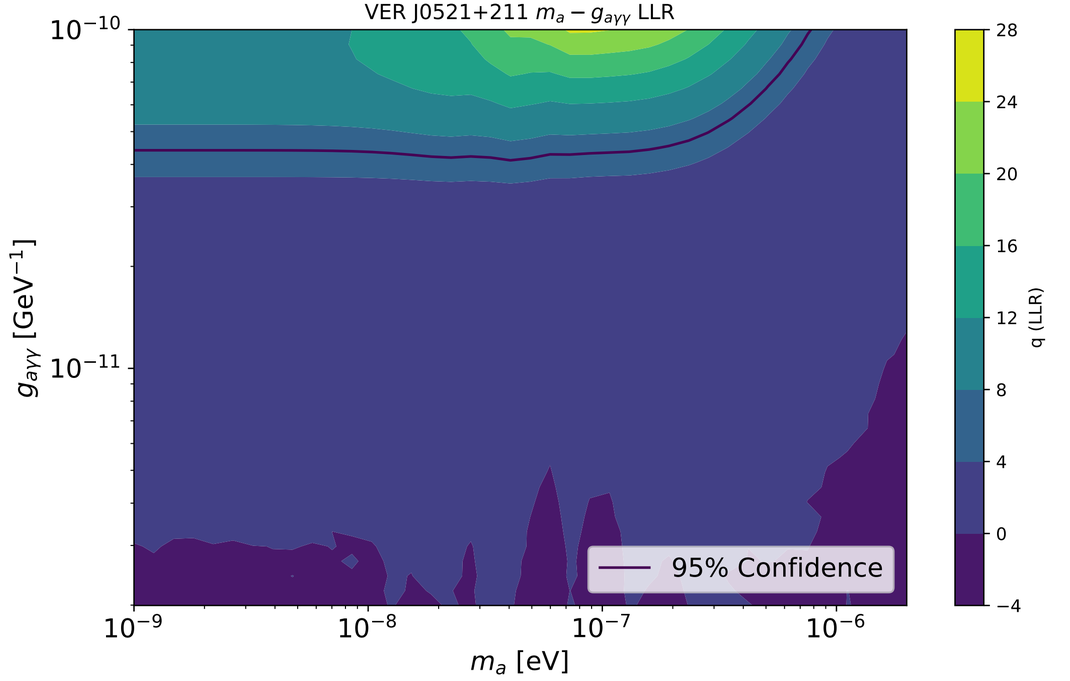

CLs Limits

$$\mathrm{CLs} = \frac{p_{s+b}}{1 - p_b}$$

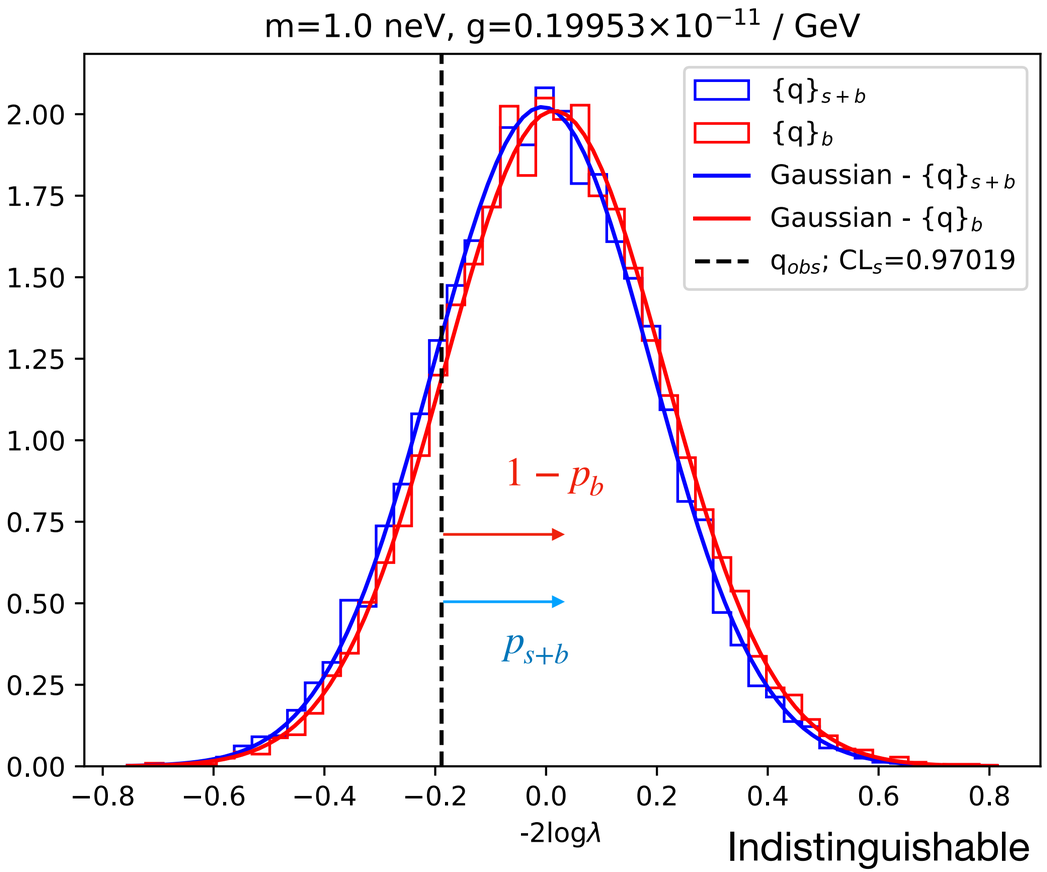

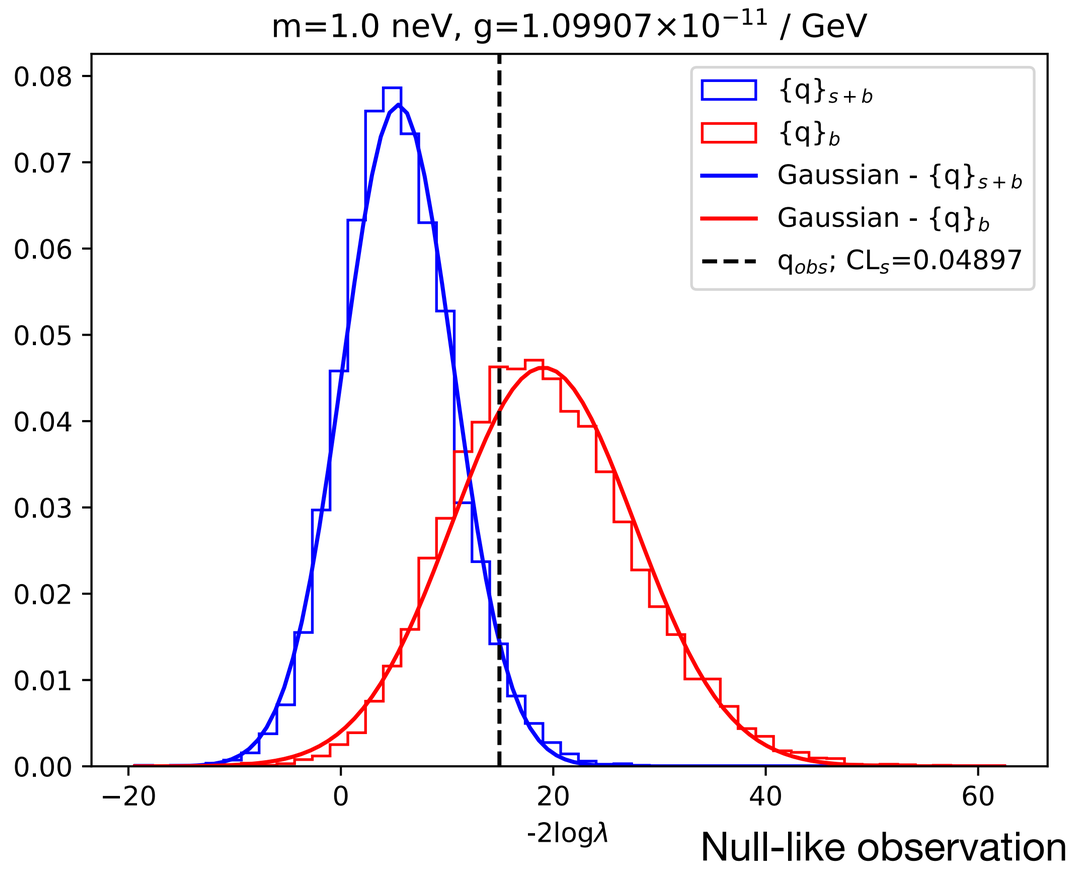

However, this analysis can be somewhat different from the typical “source finding” situation. ($n_{obs} \sim 0$)

So, CLs method divides p_{s+b} by $1 - p_b$ which panelizes rejecting hypotheses by background fluctuation.

-> It ensures that downward background fluctuations alone do not lead to overly aggressive exclusion.

CLs Limits

CLs < 0.05 for 95% CLs exclusion